Anonymous Referee #1

The authors appreciate the reviewer's encouraging, thoughtful and helpful comments and suggestions regarding the manuscript, and appreciate the time and effort spent on it.

For this particular final response, we have added specific references to line and page numbers with respect to the track change version, figure and table changes, and additional comments on top of those provided during the discussions phase. In the track change version, all deletions are marked with a ~~strikethrough~~ and all additions are marked in red.

Note that we have changed 'reflectance' to 'radiance' throughout the manuscript and use the latter in the responses to be consistent with the units reported in the AIRS visible Level 1 files (Watts/meter2/micron/steradian).**

This is a study of the relationships among cloud properties as retrieved by satellites and meteorological fields from MERRA. Most of the effort is in producing a dataset that combines AIRS/AMSU and MODIS data with MERRA at the smallest possible space and time scales. This effort is commendable and valuable, combining these data at small scales can potentially reveal a lot about the relationships between clouds and their environment. The analysis divides the data set into the four subtropical stratocumulus regions, though bigger than Klein-Hartmann regions to focus more on broken cloud regimes. Numerous quantities are examined, especially through the use of joint distributions and conditionally averaged quantities. This is mostly effective, but the weakness of the paper is that it meanders through the results without a lot of focus which I think will lose a lot of readers.

Reviewer #2 also had similar concerns. Below we describe the changes made in response to the reviewer comments.

My main suggestion is to re-work section 4, but there are probably a couple of different ways that could be done. I will include some detailed comments, some of which might become irrelevant depending on how the manuscript changes in revision.

COMMENTS:

1. While the methodology overall seems very good, I have some concerns about sample sizes and statistics. The choice to only look at 2009 must be motivated by the effort expended to gather the raw data and process down to the combined data that is being used here. Very understandable, but it is not clear whether one season of the final combined data is enough to say much.

We were indeed limited by the sheer volume of data and processing required. The full year of 2009 is processed for the entire globe. While the authors debated about presenting the full 2009 record, we concluded that the seasonal story would get lost

within the story about the four regions. Furthermore, a simple set of figures, bar charts, or tables that might show the seasonal variability could not be decided on. Also, the seasonal variability is very much sensitive to the latitude and longitude of the region selected. For instance, in the SEP region of study, during DJF (local summer), convection and tropical moist intrusions impede on the northern side of the regional box that creates systematic changes in parts of the joint pdfs. By choosing JJA in the NH and SON in the SH that correspond with peak cloud frequency as shown in Klein and Hartmann (1993), we felt we stood on the most firm ground for this investigation.

This issue might be resolved with a few words about how many samples are actually retained.

An additional column is added to Table 1 that shows the total number of data points used at the AIRS/AMSU field of regard spatial scale. Although there are slight differences in the counts between the four regions, the total number varies only slightly between ~180,000 and ~186,000 during the three-month period listed in Table 1.

We have also added the following text to the manuscript on p. 7, lines 9-11: "*The total number of collocated data points within each region is roughly ~180,000. However, the AIRS and MODIS cloud fields have smaller spatial resolutions that are aggregated to the AIRS/AMSU field of regard, and the raw counts for these fields number in the millions*."

This comment definitely applies to the joint pdfs, too. Are the color bars different for the different regions, and how much data is in a black region compared to a white region?

The gray scale/color contours are exactly the same for all regions to facilitate comparison. The gray scale indicates the log(count), where black is log(2), about 8, and white goes to log(8), about 3000. A gray scale bar at the bottom of every joint pdf figure has been added for clarity.

2. Using three moments of the reflectance is interesting, but the physical interpretation gets lost in the text.

Reviewer #2 made similar comments in regards to the connection between "cloud organization" and "skewness". We have de-emphasized "cloud organization" and replaced with "cloud variability" for several occurrences in the manuscript. We have revised the discussion of skewness in Section 4.1 in the revision.

It is made clear that skewness increases in cumulus regimes as ECF drops. Is the interpretation that this is a measure of cloud size?

With regard to the interpretation of reduced ECF because of smaller cloud size, that is a great question but we cannot provide an unambiguous answer (but we detail a

response below). There are likely several factors at play.

We have added some additional text in the middle of Section 4.1 on p. 7 lines 15-28 to highlight these issues: "*There are several factors that contribute to relationships between ECF and the various moments of radiance. A reduced ECF and increased radiance skewness (Fig. 3) may indicate smaller cloud sizes but is probably not universally true. If the cloud optical thickness is decreased, the ECF is also decreased from reductions in cloud emissivity even though cloud coverage itself may remain constant. (Recall that the ECF is a convolution of emissivity and cloud fraction.) If the cloud optical thickness is fixed, the cloud emissivity remains fixed even though the cloud coverage itself and ECF could be decreased. The ECF could also be decreased (increased) if small cloud elements become more widely spaced (packed together) assuming the cloud sizes of the individual cumulus elements remain the same. With respect to the visible radiances, the radiance is decreased if cloud elements become smaller than the nominal 2.2 km pixel size assuming the optical thickness of the cloud elements do not change. Therefore, if an increased proportion of a cloud population with normally distributed radiances becomes subpixel in size, one would expect a shift towards positive skewness. If cloud distributions are spatially resolved, an increased skewness radiance is still entirely possible if the true optical thickness of cloud distributions is skewed itself. However, in this investigation, the skewness of the MODIS optical thickness is less skewed at low ECF than visible radiance (not shown). This suggests that the skewness in the visible radiance at low ECF is at least partially caused by smaller cloud sizes.*"

The standard deviation of reflectance seems to be connected to the boundary layer depth (Fig 8 & Page 9). Is that expected? The standard deviation isn't used much except to make this point, and it is not clear that it adds much to the overall story. Maybe it would be worth extracting the standard deviation of reflectance into supplemental material?

Indeed this is the case. We have slightly modified the relevant text on p. 10 lines 7-9 to clarify that the MBL depth's relationship to the standard deviation of radiance is generally linear, while with the mean radiance it is nonlinear (the maximum MBL depth is in the middle of the joint pdf). We agree that the details of standard deviation may be explored more completely in future work. This particular point about the linearity of nonlinearity between the moments is rather interesting and worth describing, albeit briefly. We have decided to leave Figure 8 as is.

3. Section 4.2 is lacking. If I understand correctly, the point of this section is to whittle down the number of variables to look at in the later sections, settling on reflectance and ECF as the "phase space" (or maybe the "independent" or "predictor" variables?). The weakness is that the selection seems to be mostly arbitrary rather than by systematic evaluation.

We agree that the starting point for dimensionality choice appears to be pretty arbitrary in the manuscript but our approach was not. We draw upon a response to reviewer #2 to partially address this concern:

"The most honest way to go into this investigation is to ask what do we do when confronted with a choice from an enormous selection of available data? Dozens of geophysical variables are available from each instrument and reanalysis system. These variables can be plotted against each other in 1000s of combinations (or much more). The moments of these variables are also another dimensional choice, so to speak. On top of that, any field can be overlaid onto these two dimensions as done in the figures. So where does one start? As we pointed out, our reasoning for starting where we did is found here:

Line 3, page 8: "Motivated in large part to link cloud and thermodynamic properties derived from infrared and visible bands…"

In the list of comparisons, two combinations are missing that would fill in the matrix: visible reflectance and tau; ECF and cloud fraction. Both of these seem like they would exhibit strong correlations, so maybe that is why they are omitted. But in other parts of the text there is a contrast made between the MODIS and AIRS cloud fractions, so seeing ECF versus cloud fraction would be useful.

We have added these two dimensional choices to a revised version of Fig. 7. We have added them in order to enhance the discussion in the challenges of choosing the appropriate dimensionality. One combination (radiance and tau) exhibits a strong correlation while the other combination (CF versus ECF) exhibits a poor correlation. The following text has been added to the middle of Section 4.2 on page 9 lines 15-19: "*The two other panels highlight the challenges with the choice of dimensionality. In the case of radiance versus τ, while there is a strong correlation in the occurrence frequency in the more reflective clouds, the structure in the MBL depth is much less clear. In the case of cloud fraction versus ECF, the occurrence frequency is much more poorly correlated and scattered, while the MBL depth shows less structure in either dimension*."

That accounts for an assessment of the "phase space" variables, but MBL depth is also being discussed here, but it is not clear why. Is the MBL standing in here for an integrated "thermodynamic" variable?

MBL depth was chosen as a representative variable just to make the point of why the dimensions were chosen. We want to focus on dimensional choices that show structure in fields such as MBL depth. The same plots with RH, dMSE, etc. were also made and the story is very similar. The overlying quantity in the joint pdf has a larger dynamic range when ECF (infrared) and radiance (visible) is used.

4. The comparison of the regions. Early in the paper (Sections 1-3), it makes sense to look at the four regions separately. Going through Section 4, my feeling is that mostly the NEP, SEP, and SEA act very similarly, while NEA is an outlier. This is likely due to the NEA being more strongly influenced by midlatitude systems (even when filtered for mid and high clouds). A few points are raised about the difference between the hemispheres,

but it isn't clear whether there is enough sampling (especially with only one season) to make any definitive statements. So I wondered, especially at the end of Section 4.3, whether it would simplify things to combine NEP, SEP, and SEA into one population and exclude NEA or show it as a contrasting population? The advantage is to reduce figure panels and increase overall sample size at the expense of having a comparison of the regions. In the present form, I don't see that the bottom line of the paper is really emphasizing any differences in the regions except that NEA is different from the others. As a related note, the title of Section 4.3 is "Regional differences in MBL depth and dMSE," but my main takeaway from Figure 8 is the similarity of the regions, and I felt like dMSE was not much emphasized in the section.

The sample sizes are now added to Table 1 and the whitish areas of the joint pdfs have counts that number in the 100s to a few 1000s.

Thanks for the suggestion of combining the three regions. Some of the differences between the NEP, SEP, and SEA are fairly robust. For instance, the SEP and SEA have larger re, stronger u925, a more clear relationship with omega700 and omega925, and a deeper MBL than the NEP. These observations are consistent with what we currently understand about the regional differences. If the three regions are combined, these patterns will be averaged over and smoothed out. The counts in each region are found in different portions of the ECF and radiance dimensional space and will distort the patterns. (For example, the SEP has many more points at higher ECF than the NEP.) Ultimately, we are concerned that a three region joint pdf would more poorly resemble each of the three regions individually.

We have added the following text to p. 10 lines 6-7 to reiterate the reviewer's point about the similarity among three of four regions: "*Generally speaking the NEA is the largest outlier of the four regions for all radiance moments shown for MBL depth in Fig. 8 and is more affected by the midlatitudes than other regions*."

We have revised the title of Section 4.3 to "*Regional similarity in MBL depth*".

5. Comparing different scales. This study focuses on the smallest scales possible for the data, which is interesting by itself. There should be some care taken when comparing to previous studies that are explicitly working at much larger scales. This comes up in a few places in the text, but prominently at the end of section 4.3 where there is a conclusion that dMSE is correlated with small-scale spatial structure *rather than* large-scale thermodynamic structure. This might be misleading. When averaged up to longer time scales, it seems reasonable that dMSE is more representative of the large scale thermodynamic structure than the spatial structure of clouds. The same holds for LTS and EIS; the relationships between these bulk measures of inversion strength and cloud cover are only valid on relatively long time scales. Recall that the Klein-Hartmann line is derived using seasonal averages. This is discussed occasionally in the literature; one example is found in Zhang et al. (2009, DOI:10.1175/2009JCLI2891.1) where they point out that sampling the low-level divergence distribution is important for capturing the relationship between LTS and cloud cover.

Thanks for pointing out the time and spatial scale context of the agreement. In the revision, we have changed the text in question on p. 10 lines 32-33 and p. 11 lines 1-2 at the end of Section 4.3 to the following: "*This behavior is similar to MBL depth (Fig. 8f) and suggests that instantaneous values of dMSE correlate well with small-scale cloud variability. This is not inconsistent with LTS and dMSE correlating well with larger-scale atmospheric thermodynamic structure on much longer time scales.*"

6. Value of Section 4.4? The text seems to suggest that the point of this section is to compare AIRS and MERRA RH, showing they are similar and therefore useful. The MERRA RH isn't shown here (added as Figure A1), which undercuts this as the main message of the section. The section title is just "vertical structure of RH," but it is pretty hard to get a good sense for the vertical structure from the conditionally averaged contour plots showing one level at a time. The question is what aspect of the RH structure is needed to advance the overall argument of the paper? Based on Section 5, it is not clear that the vertical structure of RH is integral to the paper and Section 4.4 and Figure 10 could be deleted.

We agree with the reviewer that this section is tangential and we have eliminated it in the revision. The reason it was originally included (along with the Appendix) is that it pointed out unambiguously the nature of infrared sounding in and around clouds within the MBL. In the response during the discussions phase, we thought it might be best to combine into the Appendix and keep the figures, but after further consideration, we completely agree with the reviewer and will remove it since it does not advance the investigation.

The lines of deleted text with regard to this revision are found here: p. 4 lines 32-33; p. 5 lines 1-2; p. 8 lines 13-14 and 24-26; p. 11 lines 8-15 and 24-25; p. 14 lines 24-25; p. 15 lines 3-8; p. 16 lines 1-9.

7. The connection to microphysical effects. Section 4.5 brings r_e into the picture, and suggests that the difference between the stratocumulus and cumulus is due to microphysical processes. The next section makes the connection to wind speed, which is interesting. I'm not sure I understand the physical interpretation of the result.

The physical connection between wind speed and effective radius is drawn out more carefully in the new Section 4.4. In short, the stronger MBL wind is related to a deeper and moister MBL with more frequent precipitating clouds, which is observed as larger re in MODIS data. This could be caused by increased subpixel inhomogeneity or larger re in the cloud.

Also, it seems like making the link via the comparison of the contour plots in Figures 11 e-h and 13 e-h is a little cumbersome. Does viewing this relationship within the reflectance cloud fraction phase space make the most sense here, and if so, what do we get from this view that would not appear by directly correlating r_e and u925, for example? This seems like a key finding in the paper, and it might be better drawn out by

combining sections 4.5 and 4.6 into a more unified discussion of the r_e variation and connection to meteorology and microphysical processes.

This is a good idea and the former Sections 4.5 and 4.6 are now unified into a single Section 4.4 titled '*Relating meteorology and microphysical processes*'. Some of the front matter to the old Section 4.6 now starts this new combined section.

We contend that the radiance dimension is very useful for the discussion of r_e and meteorological variables and will leave that dimension as is for the revision. A big reason why we wanted radiance for r_e is that it is easier to point out the subpixel inhomogeneity and 3-D radiative transfer issues that arise in the highly skewed portions of the joint pdfs with low ECF that are discussed in section 4.4.

We also carried out a few additional calculations to investigate direct correlations between u_925 and reff and below we show the 2d histogram for the SEP region during SON. The binning in reff is 0.5 microns while the binning for u_925 is 0.5 m/s. The minimum count for black=10 and the maximum count for red=450.

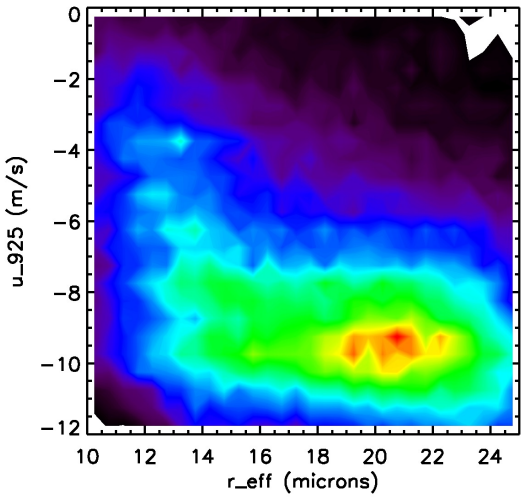

There is a relationship between u_925 and reff in the absence of other parameters such as ECF and radiance. The correlation appears to have two regimes: a more strongly sloped one at lower values of u_925 and reff, and a less strongly sloped one at higher values. We further point out that this plot is not directly comparable to the results of Figs. 10 and 12 for the same quantities because each value that populates a given bin in the above figure can be found throughout the radiance and ECF dimensions. The fact that the figures in the paper appear to show a stronger correspondence in the radiance and ECF dimensions than shown above further suggests the importance of the context of the cloud amount in which this correlation operates.

Anonymous Referee #2

We thank the reviewer for taking the time and effort to review the manuscript and appreciate the detailed and thoughtful comments. In this response, we aim to highlight more clearly the purpose, value, and novelty claimed in the manuscript.

For this particular final response, we have added specific references to line and page numbers with respect to the track change version, figure and table changes, and additional comments on top of those provided during the discussions phase. In the track change version, all deletions are marked with a ~~strikethrough~~ and all additions are marked in red.

Note that we have changed 'reflectance' to 'radiance' throughout the manuscript and use the latter in the responses to be consistent with the units reported in the AIRS visible Level 1 files (Watts/meter2/micron/steradian).**

General comment and recommendation

This manuscript presents a comparison of (correlations between) cloud properties and thermodynamic and dynamic fields derived from AIRS and MERRA data, with those derived in previous literature and derived in this paper from MODIS.

This paper is not a comparison or a validation paper. Its purpose is to describe the synergistic use of previously validated data products from AIRS, MODIS, and CloudSat, together with MERRA reanalysis at the native temporal and spatial resolution, to investigate relationships between cloud microphysical and optical properties, and dynamical and thermodynamic fields. To our knowledge, at the time of submission, we have not seen this type of approach for MBL processes. We have added the following text on p. 3 line 15-16 to clarify: "*Our primary purpose is to investigate instantaneous relationships between cloud microphysical and optical properties, dynamical, and thermodynamic variables fields from the A-train and MERRA at the native temporal and spatial resolution of the observations*."

The manuscript comes across as rather unfocused, wandering between a variety of objectives, none of which end up convincingly presented.

This is a fair statement. We have tightened up the organization of the various components in the manuscript, eliminated the RH results, trimmed some of the introduction and references, and are clearer with regard to the conclusions and take home messages.

The manuscript appears to: a) evaluate AIRS and MERRA against MODIS and other cited products;

As stated above, this paper is not a comparison, evaluation, or validation paper. In fact, the only common field used is RH between AIRS and MERRA. Section 4.4 and

Appendix A are removed from the revised manuscript per reviewer #1's suggestion and reviewer #2's concern about meandering between objectives.

AIRS, MODIS, CloudSat, and MERRA each provide unique information that can be brought to bear on observing the subtropical MBL. We are not comparing common geophysical fields obtained between them. Our guiding philosophy is "Why not play to the strengths of each instrument?" We have added text on p. 3, line 23-25: "*The satellite and reanalysis data each provide unique information that should ideally be combined together at the native resolution rather than relying on one instrument or reanalasys alone*."

b) provide physical insights into what explains the transition by means of reflectance, optical depth, boundary layer depth and effective radius;

That is (partially) correct, although there are many other geophysical variables used, and various moments (mean, variance, skewness) that highlight certain aspects of MBL structure. However, we are not attempting to "explain the transition" so much as rather present a new way to observe it, and more generally all cloud regimes (although others are beyond the scope of the investigation).

c) present the AIRS cloud product that can best reflect the transition from stratocumulus to cumulus, where a variety of measures are tried out;

There are three cloud products from AIRS that are used. (1) The AIRS cloud thermodynamic phase product is used to coarsely group together uniform stratocumulus and broken shallow cumulus. (2) The AIRS effective cloud fraction (ECF) is derived from infrared channels so it will have a different perspective of cloud cover compared to visible reflectance or optical thickness. (3) The AIRS visible channels are used to quantify the reflectance that is filtered by an AIRS visible cloud mask.

d) present different physical behaviours between four regions in which the transition between stratocumulus and cumulus occurs.

We did not attempt to explain why the four regions exhibit such differences and similarities in the transition itself. This is well beyond the scope of this investigation and would require extensive numerical modeling experiments and further investigation of several years of data. The following text has been added for clarification on p. 8 line 33 and p. 9 lines 1-2: "*While the variability within each region and between the four regions is consistent with previous studies, the physical reasons for these differences are beyond the scope of the current investigation*."

Sometimes the lack of focus and a specific question of interest seems to shines through in the authors' writing, for instance, when they introduce new sections, which might represent choices that are "not optimal", but simply provide "a fresh look at available products",

It appears the reviewer is referring to line 13, page 8 of the submitted version of the manuscript for the quoted text. We offered specific reasons for why we chose the effective cloud fraction (ECF) variable from AIRS over the cloud fraction (CF) derived from the MODIS cloud mask, and also radiance from AIRS over the optical thickness from MODIS. The reasons are described just above the quoted text:

lines 7-11, page 8: "*The MBL depth exhibits clearer patterns in the ECF dimension rather than the cloud fraction dimension. The latter is more compressed and the gradients are weaker in both dimensions. The MBL depth is deepest for lower values of ECF, τ , and reflectance. In addition, the MBL depth also decreases for the most reflective clouds at a given value of ECF while this behavior is not observed for τ . We posit that an additional population of sub-pixel cumulus clouds is captured within the reflectance data that is not captured in τ data*."

or when they describe that choosing which variables to plot in their joint pdfs is challenging.

It appears the reviewer is referring to line 2, page 8 of the submitted version of the manuscript. The most honest way to go into this investigation is to ask what do we do when confronted with a choice from an enormous selection of available data? Dozens of geophysical variables are available from each instrument and reanalysis system. These variables can be plotted against each other in 1000s of combinations (or much more). The moments of these variables are also another dimensional choice, so to speak. On top of that, any field can be overlaid onto the two dimensions as done throughout the joint pdf figures. So where does one start? As we pointed out, our reasoning for starting where we did is found here:

Line 3, page 8 (of submitted version): "*Motivated in large part to link cloud and thermodynamic properties derived from infrared and visible bands…*"

Reviewer #1 also had comments on this section under their point (3) and we have added two additional panels to figure 8. Please see this response to reviewer #1.

We have removed 'a fresh look' and modified text around p. 9 lines 21-22.

If the focus would be on presenting novel insights,

Since the reviewer is emphasizing multiple times the "novelty" of this work, after doing a word search we found only three instances of the word "novel" are used in the manuscript. This word choice is unfortunate and we have removed the three occurrences of novelty in the revision.

I had expected that beyond abstract descriptions of behavior of different quantities in the joint pdf's the authors explain what this behaviour actually tells us about observed cloud fields.

The revised Section 4.4 'Relating meteorology and microphysics' goes into detail about the behavior between multiple independent cloud variables and other properties. We show that the MODIS reff corresponds closely to u_925 and moistening and deepening of the MBL. This study is consistent with surface observations taken during the RICO campaign.

This paper is also about an attempt to describe a more holistic synthesis of the subtropical MBL from the point of view of A-train satellite observations and MERRA reanalysis built from native temporal and spatial resolution data. This paper is not about the physical causes of the stratocumulus to cumulus transition, but we do cite some of these papers in the Introduction as motivation.

If the focus would be on an evaluation of AIRS products, I would expect that the evaluation were more thorough and go beyond a comparison of seasonal averaged fields.

As stated above, this paper is not an evaluation paper for AIRS products. We have cited references throughout that point the reader to previous validation efforts that support the use of the data as shown in the manuscript.

What contributes to the wandering is that the authors use different data sets for different objectives as they present themselves.

The whole purpose of the paper is to use the different instruments and reanalysis data sets as building blocks to construct a simultaneous point of view of the MBL, playing on the strengths of each instrument. The reviewer comment strongly suggests we need to be much more clear and concise about our purpose. We hope that this concern has been resolved with the revisions.

AIRS and MERRA are used for interpreting skewness measures and the transition between cloud types, along with comparisons of MODIS. Only MODIS is used for the purpose of evaluating effective radii in the two regimes, and what might physically or methodologically explain effective radii behaviour.

As far as we are aware, MODIS has the most useful, validated, tested, and investigated global retrieval of liquid water cloud effective radius available to the scientific community. AIRS does not provide one. CloudSat uses MODIS effective radius in its forward algorithm of retrieval products. MERRA is quite awful at clouds.

In much of the authors assertions, previous literature is referenced, but often not explained.

We tried to be as comprehensive as possible with citing references for our statements. In the revision we have tried to be as clear as possible as to why we are

citing a particular work, and also eight references have been removed.

The lines of deleted text with regard to this revision are found here: p. 2 lines 17-21; p. 3 lines 5-6 and 13-14; p. 4 lines 3-5; p. 5 lines 22-23.

The deleted references are: Atkinson et al., Brient et al., Christensen et al., Nasiri et al., Platnick et al., 2003 (we keep 2017), Sandu and Stevens, Tian et al., and Vergados et al.

Because the manuscript does not present a novel insight and fails to convincingly argue for any method or the AIRS or MERRA datasets at providing novel insights, I recommend a rejection of the manuscript.

We would like to bring up that reviewer #1 had a different opinion: "This effort is commendable and valuable, combining these data at small scales can potentially reveal a lot about the relationships between clouds and their environment."

We hope that we will convince reviewer #2 the value of this work with the revisions that are made.

Specific comments

The title is unspecific (which satellite and reanalysis data sets?) and promises more insight than the paper offers. The term cloud organization is not well-chosen, because the authors do not present results on cloud organization nor discuss what cloud organization means. The words organised and disorganised are repeatedly used throughout the manuscript, but mostly in reference to organised stratocumulus and disorganised trade-wind cumulus. Both stratocumulus and trade-cumulus can be organized and disorganized, depending on some definition of organization. Sometimes it seems the authors refer to homogeneous and heterogeneous, but mostly it seems that they refer to the two different cloud types.

We have changed the title to "An A-train and MERRA view of cloud, thermodynamic, and dynamic variability within the subtropical marine boundary layer". Thus the satellite and reanalysis data are more specific and we have removed the word 'organization'.

The reviewer is entirely correct with respect to organization. That was an imprecise way to describe the data. The same exact values of mean, standard deviation, and skewness of cloud fraction, reflectance, and other fields can exhibit organization in a multitude of manners. Therefore, we will emphasize the characteristics of the moments rather than the organization. We have responded to one of reviewer #1's concerns about the use of moments under their point (2). We have added discussion regarding the interpretation of positively skewed reflectances. Please refer to this response.

The word novel is repeatedly used, but seems an overstatement. In much of the manuscript, the authors confirm insights found in previous studies, and that citation list is long.

We found the word 'novel' was used only three times in the entire manuscript and have reworded to deemphasize that the results are novel.

We argue that it is a strength of the approach taken that a long list of previous findings are reaffirmed. Given how many data sets are involved and the extensive nature of research on this topic, we think that the citation list is appropriate. Eight of the references have been removed in response to concerns from both reviewers.

One novelty that is argued for is the use of AIRS and MERRA datasets at their instantaneous native resolution. But to prove the suitability for these datasets for this kind of study, the authors qualitatively compare the morphology of the stratocumulus to cumulus transition from seasonal averaged AIRS and MERRA data with the morphology known from existing studies. I do not think a qualitative comparison of the seasonal mean transition tells us enough about how good AIRS and MERRA perform at their native resolution.

The seasonal averages were developed as a first order check on our methods from the pixel-scale instantaneous matches from which the seasonal maps were generated. The seasonal averages are one of the only ways to compare with previous studies given that the previous studies typically show seasonal maps of MBL properties.

The individual cloud and thermodynamic properties from AIRS and MODIS have been previously validated and evaluated at the pixel scale and are described in the cited references.

The authors make an argument for separating the cloud regimes stratocumulus and cumulus based on infrared-based thermodynamic phase (rather than by dynamical regime such as done in previous literature).

The motivation for this approach is found in the Methodology section. As this is a pixel based approach, we require that all ice cloud instances are removed, and we are confident that the AIRS phase product is more than sufficient and supported by the cited references about its validation and previous uses.

Page 5, lines 15-16: "*Removal of pixels containing mid- and high-level clouds helps to reduce ambiguities introduced by free tropospheric clouds and also a portion of the thermodynamic and dynamic variability associated with cloudy areas of synoptic-scale waves*."

The dynamical approach is consistent with this approach in the sense that stratocumulus clouds show larger free tropospheric subsidence than the cumulus

clouds. Below we have added a figure for the response.

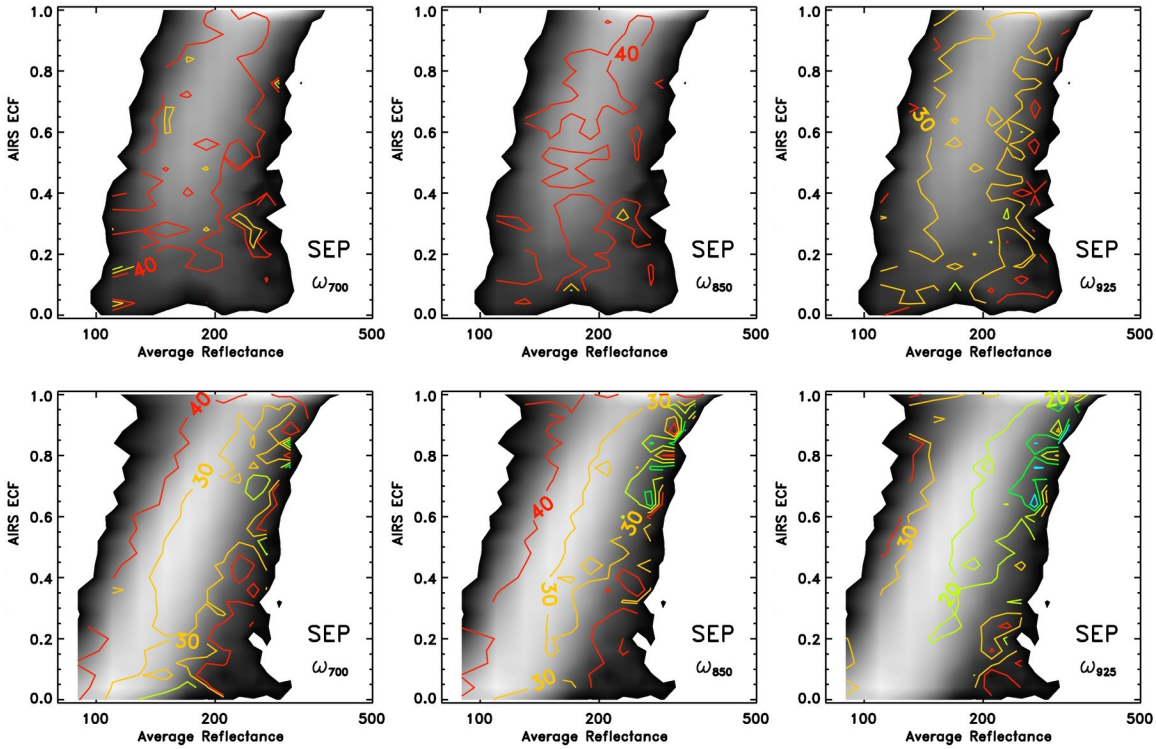

Figure caption: SEP region visible radiance versus effective cloud fraction for cumulus scenes (lower row) and stratocumulus scenes (upper row) at 700 hPa (left column), 850 hPa (center column), and 925 hPa (right column). Omega is overlaid as colored contours and is in units of hPa/day.

The omega925, omega850, and omega700 are all larger in the case of stratocumulus than cumulus. In fact, there is a gradient in omega at all three levels for cumulus in the reflectance dimension that is not observed in stratocumulus. By separating the two cloud types this gradient is observed. More reflective clouds appear to be associated with weaker subsidence in the cumulus regime.

The thermodynamic phase provides information about whether just liquid or ice is present in the detected clouds.

Based on a single scene in Figure 1 and 2 the authors argue that stratocumulus is well identified by those pixels that are detected as liquid, whereas trade-wind cumulus are those pixels that have an unknown thermodynamic phase. How do the authors know that this separation holds well for other scenes?

The granule maps in Figures 1 and 2 are shown to illustrate the data and methods. We have explored the characteristics of AIRS thermodynamic phase for the entire AIRS record and have published several papers on the topic. AIRS is a radiometrically very stable instrument with very strong sensitivity to cloud phase as discussed in Kahn et al. (2014) and Jin and Nasiri (2014) and citations within.

We refer the reviewer to page 5, lines 20-22: "*Jin and Nasiri (2014) showed that AIRS successfully identifies the presence of ice within the AIRS FOV in excess of 90% of the time when compared to CALIPSO thermodynamic phase estimates*."

After all, trade-wind cumulus are also made of liquid only, and it is unclear and not explained why they could not be identified as such in other scenes. It is also not clear for what purpose the two cloud types are separated here in this paper. Mostly this seems to be a proposition to use AIRS thermodynamic phase in future studies, but with insufficient evidence.

We agree with the reviewer that the use of the liquid and unknown phase categories is a confusing aspect of how the data is used. The delineation between stratocumulus (liquid) and cumulus (unknown) is made clearer in the revision. The following text has been added to p. 5, line 26-31: "*As the AIRS cloud phase algorithm is based on a channel selection that exploits differences in the index of refraction for liquid and ice, it is possible that the cloud amount observed in the AIRS pixel is small enough the spectral signature is small such that it does not trigger a positive liquid test (e.g., Jin and Nasiri, 2014). The ECF for these unknown phase cases can be above the sensitivity of cloud detection (validated using CALIPSO lidar, see Kahn et al., 2014). As a result, none of the phase tests are triggered even though a small amount of cloud is found in the AIRS pixel. These unknown cases line up very well with the frequency of trade cumulus in the four regions selected*."

One aspect of the paper that prevents it from providing clear physical insights (if this were the main objective) is that the authors never explain what the skewness in reflectance or optical depth tells us about the nature of the cloud field that is observed (and this is true for many of the behaviours derived from the joint pdfs). The skewness measure has been used in previous studies, and can with some background of course be interpreted, but the authors never explicitly do. This makes the description of results rather abstract.

We agree with the reviewer that this is a weakness in the paper. Thus, we have strengthened this aspect of the interpretation of the data. On the whole, the more skewed the reflectance is, the smaller the ECF is. When the reflectance is approximately Gaussian, the ECF is larger. The former is seen very clearly in the cumulus pdfs and the latter in the stratocumulus pdfs. Since there is such good separation between the two cloud types, they should be discussed separately. This also should be considered as an independent confirmation of the sensitivity of the AIRS phase algorithm to cloud type.

Even for the same combination of reflectance and ECF in cumulus and stratocumulus pdfs for the MBL depth, the MBL depth is shallower for stratocumulus. The same is true for dMSE (more positive for stratocumulus than trade cumulus.) This is a really interesting result that shows there is cloud regime dependence even for the same value of ECF and reflectance, and that separation is

facilitated by the AIRS phase algorithm categories liquid and unknown.

The text has been revised accordingly. As reviewer #1 had similar concerns, please refer to the response to reviewer #1 under point (2) for additions and changes made to the manuscript.

The discussion in section 4.5 and the conclusions argue for both physical causes (precipitation) as well as retrieval-related biases (inhomogeneity) for the observed larger effective radius in cumulus clouds compared to stratocumulus. But whereas first is stated that (L24) "the observed increase in re is entirely consistent with environmental variability (winds/droplet growth/precipitation)", it is written further along that the greater inhomogeneity in such precipitating cumulus fields can cause assumptions used in retrievals to break down. Hence, should I trust the retrieved larger effective radii observed?

The work of Cho et al (2015) goes into great detail on the failures in the MODIS re retrievals and the various causes. The factors that cause the failed retrievals, discussed in Cho et al., are also operating within the successful retrievals described in this paper. The bottom line is that the pixel-scale inhomogeneity is producing larger values of re for successful retrievals that are correlated with increased MBL wind and precipitation frequency. Cloud inhomogeneity is correlated to precipitation and that is a big reason why the re increases. However, the actual cloud droplets can be larger too. The underlying assumption about the cloud droplet size distribution may also be problematic and other factors may come into play. Teasing apart these effects warrants significant research efforts; these questions are being pursued by the MODIS algorithm team.

We have made several modifications to the new Section 4.4 that includes discussion of re and its interpretation:

p. 11, lines 30-31: "*Figure 10 shows the MODIS derived r_e for stratocumulus (Fig. 10a-d) and cumulus (Fig. 10e-p) that are limited to successful retrievals (no PCL pixels are included).*"

p. 12, lines 3-4: "*Cloud inhomogeneity may also lead to significant 3-D radiative transfer effects but these tend to cause both larger and smaller r_e in similar proportions (Zhang et al., 2012).*"

p. 12, lines 11-15: "*One general interpretation of the larger r_e in cumulus (Fig. 10e-h) when contrasted to stratocumulus (Fig. 10a-d) is that it is caused by increased inhomogeneity of cumulus (Zhang et al., 2012), retrieval failures and partly cloudy pixels (Cho et al., 2015), and view angle biases (e.g., Liang et al., 2015) that are further coupled together with other factors at play (Zhang et al., 2016). The aforementioned issues may still impact a successful r_e retrieval.*"

p. 12, lines 20-22: "*Successful retrievals with pixels that have increased subpixel*

***horizontal inhomogeneity may be more frequently precipitating, either because of larger r_e in the cloud, or because the plane parallel homogeneous bias is larger in precipitating clouds*.**"

p. 15, lines 13-15: "*This may be caused by larger r_e in the cloud itself or that precipitating clouds are associated with an increased subpixel inhomogeneity that leads to the plane parallel homogeneous bias; this topic warrants further investigation*."

The lines of deleted text with regard to this revision are found here: p. 4 lines 21-23; p. 15 lines 15-19.

In the last paragraphs of section 4.6 and the summary, the authors argue two seemingly contradicting statements with which they end their manuscript. Namely, that three of the four regions studied show similar relationships and behaviours among cloud-related quantities and the (thermo)dynamic state, but also that the relationships are non-unique (can vary greatly), for which their datasets provide a good opportunity for further exploration. I understand the subtlety, but is this the best ending?

We agree that this isn't the most useful of endings. We have revised in the end of the new Section 4.4 (which was previously Section 4.6) and removed the sentence in question. In the summary, we have removed the last two sentences. Now the summary ends with the following short paragraph on future work on p. 15, lines 28-31: "*Future work will expand to other cloud regimes, additional data sets, and multiple years of data. A similar approach with numerical model output should also be attempted using temporal snapshots of similar geophysical fields. We expect that this approach will be especially useful for linking cloud microphysics together with the thermodynamic and dynamic state of the atmosphere at the process scale."*

An A-train and MERRA ~~A satellite and reanalysis~~ view of cloud ~~organization~~, thermodynamic, and dynamic variability within the subtropical marine boundary layer

Brian H. Kahn[1], Georgios Matheou[1], Qing Yue[1], Thomas Fauchez[2], Eric J. Fetzer[1], Matthew Lebsock[1], João Martins[3], Mathias M. Schreier[1], Kentaroh Suzuki[4], and João Teixeira[1]

[1] Jet Propulsion Laboratory, California Institute of Technology, Pasadena, CA, USA
[2] NASA Goddard Space Flight Center, Greenbelt, MD, USA
[3] Instituto Português do Mar e da Atmosfera, Lisbon, Portugal
[4] Atmosphere and Ocean Research Institute, The University of Tokyo, Kashiwa, Japan

Correspondence to: Brian H. Kahn (brian.h.kahn@jpl.nasa.gov)

Abstract. The global-scale patterns and covariances of subtropical marine boundary layer (MBL) cloud fraction and spatial variability ~~organization~~ with atmospheric thermodynamic and dynamic fields remain poorly understood. We describe an ~~a novel~~ approach that leverages coincident NASA A-train and the Modern Era Retrospective-Analysis for Research and Applications (MERRA) data to quantify the relationships in the subtropical MBL derived at the native pixel and grid resolution. Four subtropical oceanic regions that capture transitions from ~~closed cell~~ stratocumulus to ~~open cell~~ trade cumulus are investigated. We define stratocumulus and cumulus regimes based exclusively from infrared-based thermodynamic phase. Visible radiances ~~reflectances~~ are normally distributed within stratocumulus and are increasingly skewed away from the coast where ~~disorganized~~ trade cumulus dominates. Increases in MBL depth, wind speed and effective radius (r_e), and reductions in 700-1000 hPa moist static energy differences and 700 an 850 hPa vertical velocity, correspond with increases in visible radiance ~~reflectance~~ skewness. We posit that a more robust representation of the cloudy MBL is obtained using visible radiance ~~reflectance~~ rather than retrievals of optical thickness that are limited to a smaller subset of cumulus. An increase in r_e within shallow cumulus is strongly related to higher MBL wind speeds that further correspond to increased precipitation occurrence according to CloudSat. Our results are consistent with surface-based observations and suggest that the combination of A-train and MERRA data sets have potential to add global context to our process understanding of the subtropical cumulus-dominated MBL.

1 Introduction

Much of the uncertainty in projections of future climate is directly or indirectly related to clouds and their associated processes (IPCC AR5, 2013) including shallow marine cumuliform clouds (Bony and Dufresne, 2005). The low cloud-climate feedback is generally regarded to be positive (e.g., Clement et al., 2009). Many studies however suggest that the sign

and magnitude of the feedback are cloud-type dependent (e.g., Caldwell et al. 2013; Bretherton et al., 2013; ~~Brient and Bony, 2013;~~ Dal Gesso et al., 2015; Stephens, 2005; Yue et al., 2017~~2016~~; Zelinka et al., 2012).

Using large eddy simulation (LES) experiments forced with doubled CO_2, Bretherton et al. (2013) show that the gradient of RH from the MBL to the free troposphere is a key factor that controls the shortwave cloud radiative feedback. Rieck et al. (2012) used LES forced by perturbed lower tropospheric temperature profiles with fixed RH to show that an increase in surface moisture fluxes leads to a drying of the trade cumulus-topped MBL. The drying overwhelms the increased shortwave reflection from the liquid water lapse rate feedback, thus leading to reduced cloudiness and a positive shortwave cloud feedback. These mechanisms are also discussed by Nuijens and Stevens (2012) in the context of bulk theory and clearly demonstrate that free tropospheric temperature and moisture gradients act as constraints for climate change-induced surface flux changes.

While the constant RH framework is a useful concept to investigate cloud-climate feedback in simplified modeling experiments, an overall reduction of RH in the subtropical free troposphere was found in the CMIP3 (Sherwood et al., 2010; Fasullo and Trenberth, 2012) and CMIP5 (Lau and Kim, 2015) archives with a non-negligible spread in the changing magnitude and vertical structure of RH among the models. Therefore, the assumption that constant RH might hold across the diversity of subtropical cloud regimes with a changing climate is likely not valid. Medeiros and Nuijens (2016) showed that the RH gradient between the MBL and lower free troposphere is widely variable among the CMIP5 models within the trade cumulus regime. ~~Sandu and Stevens (2011) show that the rate at which the transition from stratocumulus to trade cumulus occurs is modulated by downwelling longwave flux that is in part driven by free tropospheric humidity variations, but the overall morphology of the transition is fairly insensitive to the humidity. Christensen et al. (2013), Bretherton et al (2013), and other works confirm the importance of free tropospheric moisture on the MBL through increased downward longwave emission that helps modulate the rate of cloud top entrainment.~~ Therefore, further examination of cloud variability ~~organization~~ and the vertical structure of RH with present-day satellite and reanalysis observations is warranted.

A strong linkage between cloud amount and EIS (Wood and Bretherton, 2004), lower tropospheric stability (LTS) (Klein and Hartmann, 1993), and moist static energy differences (dMSE) between the free troposphere and surface (Kawai and Teixeira, 2010; Chung et al., 2012; Kubar et al., 2015) is well understood. Satellite observations of the MBL have revealed prodigious variations of cloud organization that span orders of magnitude over spatial and temporal scales (Cahalan et al., 1994; ~~Atkinson and Zhang, 1996;~~ Wood and Hartmann, 2006; Muhlbauer et al., 2014). Even for a fixed value of cloud fraction, a large diversity of statistical variability ~~cloud spatial organization~~ may be observed (Kawai and Teixeira, 2012). Correlations of cloud fraction to other environmental variables are highly dependent on the time scale of comparison (e.g., Brueck et al., 2015). At present, the relationships of cloud fraction and spatial variability ~~organization~~ to larger-scale properties other than EIS/LTS remain poorly understood. Furthermore, previous work has emphasized correlations of MBL cloud properties to 500 hPa vertical velocity and RH that are averaged over monthly, seasonal, or annual time scales. Kawai and Teixeira (2010) found significant correlations for instantaneous observations of cloud inhomogeneity and the skewness

of LWP to thermodynamic structure changes between 850 and 1000 hPa; the correlations are larger for LWP than with cloud fraction.

Modeling and observational studies have demonstrated that that the vertical structures of moments of conserved thermodynamic variables depend on the cloud regime (e.g., Suselj et al., 2013; Ghate et al., 2016;~~)~~. Zhu and Zuidema, ~~(~~2009). ~~used cloud-resolving models forced by field campaign data to quantify the statistical variability of thermodynamic and dynamic properties of the subtropical MBL. There are~~ s Substantial differences exist between stratocumulus and trade cumulus in the mean, variance, skewness, and kurtosis of equivalent potential temperature θ_e, liquid water potential temperature θ_l, and vertical velocity profiles~~.~~, ~~The differences that exist among the modeled cloud regimes~~ and point to the importance of ~~obtaining~~ a global perspective uniquely provided by satellite and reanalysis data. The NASA A-train (Stephens et al., 2002) provides a wealth of remote sensing data about the microphysics and thermodynamics of the cloudy MBL. ~~Model r~~Reanalysis data such as the Modern Era Retrospective-Analysis for Research and Applications (MERRA; Rienecker et al., 2011) offer a complementary set of thermodynamic and dynamic variables that help establish a larger-scale perspective for coincident remote sensing observations. ~~Reanalysis data is typically used in the context of gridded monthly, seasonal or annual means and the native spatial and temporal resolution available has not been well explored at this point.~~

Our primary purpose is to investigate instantaneous relationships between cloud microphysical and optical properties, dynamical, and thermodynamic variables fields from the A-train and MERRA ~~We describe a method that blends together the reanalysis and remote sensing data sets~~ at the native temporal and spatial resolution of the observations. ~~This approach has been successfully implemented in reconciling multiple satellite cloud products (Nasiri et al., 2011) and improving the robustness of satellite radiance inter-comparisons (Schreier et al., 2010).~~ The matching approach uses a nearest neighbor technique weighted by the sensor spatial response function (Schreier et al., 2010). The mean, variance, and skewness of MODIS cloud properties at 1-km or 5-km resolution is retained within a larger 45-km resolution Atmospheric Infrared Sounder (AIRS)/Advanced Microwave Sounding Unit (AMSU) field of regard (FOR), while MERRA's 1/2° × 2/3° resolution thermodynamic and dynamic variables are matched to the nearest AIRS/AMSU FOR. The satellite and reanalysis data each provide unique information that should ideally be combined together at the native resolution rather than relying on one instrument or reanalasys alone. The geophysical fields are retained at the native spatial and temporal resolution such that the instantaneous "snapshots" of the cloud probability density function (pdf) are preserved and are then conditioned by available thermodynamic and dynamic variables. The statistical behavior of cloud properties ~~and their spatial organization~~, and how the thermodynamic and dynamic state variables are related to them, are inferred using the finest temporal and spatial resolutions available.

Section 2 describes the data sets used while Section 3 details the methodological approach taken in this investigation. Section 4 details the results, beginning with a regional spatial context, then concluding with examination of joint pdfs. We conclude in Section 5.

2 Data

The AIRS/AMSU sounding suite located onboard NASA's EOS Aqua satellite has obtained vertical profiles of temperature and water vapor at approximately 45-km horizontal resolution since September 2002 (Chahine et al., 2006). ~~Kalmus et al. (2015) describe comparisons of AIRS temperature and water vapor profiles to radiosondes launched during the Marine ARM GPCI of Clouds (MAGIC) campaign and ECMWF analysis data.~~ While AIRS cannot capture the sharpness of the temperature and water vapor mixing ratio gradients across the top of the MBL (Maddy and Barnet, 2008; Yue et al., 2011), the coarse-resolution vertical gradients from the surface to the lower free troposphere are obtained with high fidelity (Yue et al., 2013; Kalmus et al., 2015). The AIRS operational products also provide numerous cloud variables that include effective cloud fraction (ECF), cloud thermodynamic phase (liquid, ice, and unknown categories), and others (Kahn et al., 2014). A MBL depth estimate inferred from the height/pressure of maximum RH gradient is described and validated with radiosondes launched during the Rain in Shallow Cumulus over the Ocean (RICO) campaign in Martins et al. (2010).

The Version 5 AIRS channel 4 visible spectral radiance ~~reflectance~~ (0.49–0.94 μm) (Gautier et al., 2003; Aumann et al., 2006) with a nadir spatial resolution of 2.28 km is used and has units of W/m^2/μm/sr. AIRS visible band data is co-registered to the AIRS IR footprint such that 72 visible pixels are aligned within every footprint. A prototype AIRS visible cloud mask (Gautier et al., 2003) that was developed to support earlier algorithm development efforts is also used. Although the cloud mask has not been compared directly against benchmarks such as the MODIS cloud mask, manual inspection suggests that this cloud mask tends towards ~~is~~ clear-sky conservative and captures many shallow, broken sub-pixel cumulus clouds.

The Moderate Resolution Imaging Spectroradiometer (MODIS) instrument on EOS Aqua is capable of observing a wide variety of land, ocean, and atmospheric variables (Platnick et al., ~~2003,~~ 2017) that are co-located to the AIRS FOV ~~(Schreier et al., 2010)~~. We use the Collection 6 ~~5.1~~ liquid phase cloud optical thickness τ and effective radius r_e retrievals from the MYD06_L2 swath product and the 1-km cloud mask from the MYD035_L2 swath product. ~~Zhang et al. (2012, 2016) and Cho et al. (2015) have shown that the retrievals behave well within homogeneous clouds but contain biases along cloud edges and within partly cloudy pixels where 3-d radiative effects become important and algorithmic assumptions are challenged.~~ Platnick et al. (2017) show that the r_e ~~re~~ change between C5.1 and C6 is ±1–2μm. We have tested the differences in the pdfs between C5.1 and C6 for a subset of the data investigated and very little change in the pdfs were observed (not shown). The MODIS liquid cloud r_e is used as a proxy for precipitation and is verified with the CloudSat 2C-RAIN-PROFILE (Release 4) precipitation product (L'Ecuyer and Stephens, 2002).

The MERRA instantaneous, six-hourly, native-resolution, gridded data sets at 1/2° × 2/3° (Rienecker et al., 2011) are used to assess the thermodynamic profiles derived from AIRS, assign vertical profiles of horizontal u and v wind components, and vertical profiles of pressure velocity ω in the MBL and lower free troposphere. All of the instantaneous MERRA data are spatially and temporally matched to the A-train orbit using a nearest neighbour matching approach with no time interpolation. ~~Previous investigations have compared climatological averages of MERRA against AIRS (Tian et al., 2013) and GPS RO (Vergados et al., 2015) in the subtropical MBL. Instantaneous, cloud regime comparisons to AIRS have not~~

~~been attempted until the present investigation and the value of this approach is demonstrated in Section 4. We use the 1000, 925, 850, and 700 hPa levels to compare to the AIRS Standard Level 2 product.~~

3 Methodology

Four subtropical oceanic regions that capture transitions from ~~organized closed-cell~~ stratocumulus to ~~disorganized open-cell~~ trade cumulus are investigated ~~(Muhlbauer et al., 2014)~~. The four regions are greatly expanded in scale from those used in Klein and Hartmann (1993) to investigate the stratocumulus-topped MBL and are listed in Table 1. While all available daytime (ascending) orbits from 1 January 2009 to 31 December 2009 were used ~~analyzed in all regions~~, the remaining discussion is limited to the seasons that contain the observed peak in cloud frequency listed in Table 1 (Klein and Hartmann, 1993).

Figure 1a is an example visible image for a six-minute AIRS granule within the southeast Atlantic Ocean (SEA). The visible band captures various spatial structures of clouds ~~scales of organization~~. The cloud mask derived from AIRS visible bands for the same granule is shown in Fig. 1b. The cloud mask is used to narrow down the spatial sampling for the following analysis. The cloud mask likely includes instances of clear sky, but the approach only requires a coarse masking approach to filter out a majority of the clear sky pixels. We will discuss implications regarding the filtering process in Section 4.

Removal of pixels containing mid- and high-level clouds helps to reduce ambiguities introduced by free tropospheric clouds and also a portion of the thermodynamic and dynamic variability associated with cloudy areas of synoptic-scale waves. Figure 2 shows the AIRS infrared T_b within a clean atmospheric window at 1231 cm^{-1}, the cloud thermodynamic phase mask, three constant pressure levels of AIRS RH (700, 850, and 925 hPa), and the skewness of visible radiance ~~reflectance~~ for the same granule shown in Fig. 1. The cloud thermodynamic phase identifies some scattered ice in the northern portion of the granule. All pixels identified with ice are removed in the following analysis. Jin and Nasiri (2014) showed that AIRS successfully identifies the presence of ice within the AIRS FOV in excess of 90% of the time when compared to CALIPSO thermodynamic phase estimates. ~~The rate of agreement depends on the complexity of the vertical structure and horizontal heterogeneity (Jin and Nasiri, 2014).~~ A similar approach is taken in Nam et al. (2012) and Myers and Norris (2015) to minimize impacts from convection and synoptic-scale weather systems. Additional occurrences of $T_{b,1231} < 273$ K that potentially contain supercooled liquid phase mid-level clouds are also removed ~~in the following analysis~~.

As the AIRS cloud phase algorithm is based on a channel selection that exploits differences in the index of refraction for liquid and ice, the cloud amount observed in the AIRS pixel is frequently small enough that the spectral signature does not trigger a positive liquid test (e.g., Jin and Nasiri, 2014). The ECF for these unknown phase cases can simultaneously be well above the sensitivity of cloud detection (validated using CALIPSO lidar, see Kahn et al., 2014). As a result, none of the phase tests are triggered even though cloud is observed within the AIRS pixel. These unknown cases line up very well with the frequency of trade cumulus in the four regions selected.

The AIRS liquid detections coincide with uniform stratocumulus (Fig. 1) with close to normally distributed visible radiances ~~reflectances~~ (lower right, Fig. 2), while unknown detections correspond well to ~~disorganized~~ shallow cumulus ~~(Muhlbauer et al., 2014)~~ with a distinctive positively skewed visible radiance ~~reflectance~~, very similar to previous results obtained using liquid water path (LWP) (Wood and Hartmann, 2006; Kawai and Teixeira, 2010). Previous investigations have used free tropospheric vertical velocity to separate cloud regime types (e.g., Bony and Dufresne, 2005; Medeiros and Stevens, 2011; Nam et al., 2012). Henceforth, the two regimes defined exclusively by *liquid* and *unknown* phase detections will be generically referred to as *stratocumulus* and *cumulus* regimes, respectively. An advantage of this approach is that the temporal and spatial variations of cumulus and stratocumulus cloud areas are more precisely separated from each other.

For the AIRS/AMSU FORs containing MBL clouds, we collocate the coincident AIRS and MODIS geophysical fields are collocated. The AIRS ECF is averaged over the entire AIRS/AMSU FOR where clear sky is equal to a value of zero. The AIRS thermodynamic phase is averaged over cloudy AIRS FOVs only. The individual phase tests are summed and ~~we define~~ liquid is defined for values < -0.8, unknown between -0.8 to +0.8, and ice for values > +0.8. The MODIS cloud mask and τ are averaged over the entire AIRS/AMSU FOR. The MODIS r_e is averaged only over the successful retrievals that are a subset of MODIS pixels identified as containing cloud. The nearest neighbour is matched for MERRA geophysical fields at a similarly sized ~~(or larger)~~ spatial resolution. The mean, standard deviation, and skewness of MODIS and AIRS FOV ~~cloud~~ properties~~, visible reflectance, and infrared radiance~~ are then calculated for each AIRS/AMSU FOR separately. Therefore, multiple satellite instrument and reanalysis observations at multiple spatial scales can be linked together through joint pdfs for a large combination of statistical moments. These data serve as the basis of the following investigation.

4 Results

In Section 4.1, regional-scale, seasonal averages are calculated from the pixel-scale data described in Section 3 for 90 daytime (130 pm equatorial crossing time) snapshots and are then re-gridded to 1°×1° spatial resolution. In Section 4.2, multivariate pdfs are investigated in the context of limiting the plethora of choices among variables and statistical moments. In Sections 4.3 and 4.4~~-4.6~~, several sets of thermodynamic and microphysical pdfs are quantified and described.

4.1 Regional spatial averages

Figure 3 shows the visible radiance ~~reflectance~~ skewness for JJA in the NEP and NEA regions, and SON in the SEP and SEA regions~~,~~ with an overlay of AIRS total ECF. The coastal stratocumulus radiances ~~reflectances~~ are distributed approximately normally while the radiances ~~reflectances~~ are positively skewed away from the coast where disorganized cumulus dominates (e.g., Wood and Hartmann, 2006). Contours of the magnitude of radiance ~~reflectance~~ skewness closely align to the magnitude of ECF in cumulus while much less so in proximity to the coast within stratocumulus. Very poor spatial correspondence between radiance ~~reflectance~~ skewness and the mean value of MODIS cloud fraction was found (not shown) and is consistent with low correlations between GOES derived cloud fraction and LWP noted by Kawai and Teixeira

(2010) in the SEP region. Interestingly, the average radiance ~~reflectance~~ skewness is larger and ECF is smaller in the NEP than the other three regions and is consistent with other satellite observations (Klein and Hartmann, 1993; Rossow and Schiffer, 1999) and surface-based observations (Wood, 2012). The patterns of radiance ~~reflectance~~ skewness shown in Fig. 3 also resemble typical climatological patterns of cloud sizes reported in Wood and Field (2011) and cloud texture as viewed from the Multi-angle Imaging SpectroRadiometer (MISR) (Zhao et al., 2016).

Values of MODIS total water path (TWP) skewness do not show a clear transition from normally distributed to positively skewed values in ~~(~~Weber et al.~~,~~ ~~(~~2011). This further motivates the removal of mid- and high-level cloud occurrences using the AIRS phase mask that comprise anywhere from 4 to 18% of the total number of FOVs depending on the region of study (Table 1). The total number of collocated data points within each region is roughly ~180,000. However, the AIRS and MODIS cloud fields have smaller spatial resolutions that are aggregated to the AIRS/AMSU field of regard, and the raw counts for these fields number in the millions. Oreopoulos and Cahalan (2005) show that the inhomogeneity parameter calculated from MODIS LWP, rather than TWP, is most homogeneous near the coast and indicates increasing heterogeneity that extends into the cumulus regimes. We argue that the results of Oreopoulos and Cahalan (2005) are more definitive than those shown in Weber et al. (2011) and more closely resemble the gradients and magnitudes contained within Fig. 3.

There are several factors that contribute to relationships between ECF and the various moments of radiance. A reduced ECF and increased radiance skewness (Fig. 3) may indicate smaller cloud sizes but is probably not universally true. If the cloud optical thickness is decreased, the ECF is also decreased from reductions in cloud emissivity even though cloud coverage itself may remain constant. (Recall that the ECF is a convolution of emissivity and cloud fraction.) If the cloud optical thickness is fixed, the cloud emissivity remains fixed even though the cloud coverage itself and ECF could be decreased. The ECF could also be decreased (increased) if small cloud elements become more widely spaced (packed together) assuming the cloud sizes of the individual cumulus elements remain the same. With respect to the visible radiances, the radiance is decreased if cloud elements become smaller than the nominal 2.2 km pixel size assuming the optical thickness of the cloud elements do not change. Therefore, if an increased proportion of a cloud population with normally distributed radiances becomes subpixel in size, one would expect a shift towards positive skewness. If cloud distributions are spatially resolved, an increased skewness radiance is still entirely possible if the optical thickness of cloud distributions is skewed itself. However, in this investigation, the skewness of the MODIS optical thickness is less skewed at low ECF than visible radiance (not shown). This suggests that the skewness in the visible radiance at low ECF at least partially arises from smaller cloud sizes.

The mean MBL depth (Fig. 4) reaffirms a characteristic transition from shallow MBLs (920–970 hPa) near the coast to deeper MBLs (830–880 hPa) to the west and is a well-observed feature of the stratocumulus to cumulus transition previously observed by ~~(~~Karlsson et al.~~,~~ (2010)~~;~~ Teixeira et al.~~,~~ (2011), and others. Closest to the coast, the MBL is shallowest in the NEA and slightly deeper in the NEP. The SEA and SEP are deeper than their NH counterparts with SEP the deepest. The SEP MBL depths agree with VOCALS-REx in situ radiosonde-derived temperature inversion base heights described by

(Bretherton et al., (2010). Furthermore, the inter-regional differences in MBL depth show consistency with global positioning system-radio occultation (GPS-RO) data described by (Chan and Wood, (2013).

Differences in the moist static energy (dMSE) between 700 and 1000 hPa are calculated following the approach outlined by Kubar et al. (2012) and are shown in Fig. 4. The dMSE is calculated from quality-controlled AIRS soundings (PGood ≥ 1000 hPa) and is nearly identical to estimates from ERA-Interim shown by (Kubar et al., (2012). The magnitude of dMSE is larger and positive near the coast in the SH compared to the NH and is somewhat reduced in the NEA region. Yue et al. (2011) showed that values of EIS and LTS obtained from AIRS soundings are lower in the NEA compared to the other three regions and are also consistent with Fig. 4.

Seasonal averages of AIRS RH_{700} with an overlay of the corresponding MERRA-AIRS RH_{700} differences are shown in Fig. 5. Wind vectors depict the mean horizontal flow. Overall, RH_{700} in the SH is lower than the NH while the NEA is the moistest of the four regions and SEP the driest. MERRA is on average moister than AIRS by ~5% in the NH, nearly identical to AIRS in the SEA, and a much more spatially heterogeneous difference is observed in the SEP from the coastal proximity westward between 8–12°S. ~~Tian et al. (2013) showed that at 700 hPa, MERRA is typically biased wet compared to AIRS in the NEP and NEA and a more complicated spatial pattern in the SEP that is consistent with Fig. 5.~~

Bretherton et al. (2010) demonstrate that the free troposphere in the SEP westward of 75°W is characteristically very dry (0.1 g kg^{-1}) with sporadic filaments of moist air (as high as 3-6 g kg^{-1}) up to an altitude of 2.5 km. In addition, these moist filaments have been observed with GPS-RO refractivity profiles by (von Engeln et al., (2007). The vertical structure of RH obtained from VOCALS-REx radiosondes implies a well-mixed MBL near the coast with MBL decoupling west of 80°W. Myers and Norris (2015) showed that 700 hPa is drier in the SH subtropics compared to the NH using ERA-Interim data. When GCMs are sampled for RICO-like conditions using representative mid-tropospheric large-scale vertical velocities as in (Medeiros and Stevens, (2011), a dry bias is obtained above the MBL in comparison to a composite of RICO radiosondes.

The seasonal averages of AIRS RH_{850}, and the corresponding MERRA-AIRS RH_{850} differences, are larger than that found for RH_{700} (Fig. 6) and are due to temperature and water vapor weighting function widths on the order of 2–3 km (Maddy and Barnet, 2008). ~~While the MBL is typically deepest in the SEP, the magnitude of RH_{850} is lower compared to the NEP and is further evidence for a drier and warmer lower free troposphere in the SEP. The MERRA-AIRS differences are -5% to -10% in the NEA, while they are mostly positive and up to +15% in the NEP, SEP, and SEA.~~

In summary, the seasonal averages exhibit realistic three-dimensional spatial morphologies and gradients and show consistency with MERRA RH in the subtropical MBL. The MBL depth and seasonal variations (not shown) agree with GPS-RO (Chan and Wood, 2013). The AIRS-derived dMSE between 700 and 1000 hPa agrees with ERA-Interim (Kubar et al., 2012). The radiance ~~reflectance~~ skewness is strongly related to ~~cloud organization and~~ dMSE (Kawai and Teixeira, 2012). The AIRS ECF distributions closely correspond to well-established climatologies of cloud amount (e.g., Klein and Hartmann, 1993; Rossow and Schiffer, 1999; Wood, 2012). The vertical structure of the horizontal wind flow well represents known climatological patterns in the MBL and lower free troposphere. While the variability within each region

and between the four regions is consistent with previous studies, the physical reasons for these differences are beyond the scope of the current investigation.

In the following sub-sections, an ensemble of multivariate and multi-moment pdfs are examined~~, and novel insights on the structure of the cloud topped subtropical MBL will be discussed~~.

4.2 Dimensionality of multivariate pdfs

Choosing an ideal subset of variables and statistical moments to form the basis of joint histograms is a ~~great~~ challenge. Motivated in large part to link cloud and thermodynamic properties derived from infrared and visible bands, we describe six ~~four~~ variable combinations~~: (1) visible reflectance versus ECF; (2) τ versus ECF; (3) visible reflectance versus cloud fraction; and (4) τ versus cloud fraction~~. The natural log frequency of occurrence ~~for the four combinations~~ is shown in gray scale from black to white and MBL depth is superimposed as ~~colored and labelled~~ contours (Fig. 7).

The MBL depth exhibits clearer patterns in the ECF dimension (Fig. 7a,c) rather than the cloud fraction dimension (Fig. 7b,d). The latter is more compressed and the gradients are weaker in both dimensions. The MBL depth is deepest for lower values of ECF, τ, and visible radiance ~~reflectance~~. In addition, the MBL depth also decreases for the most reflective clouds at a given value of ECF while this behavior is not observed for τ. ~~We posit that~~ a An additional population of sub-pixel cumulus clouds is captured within the radiance ~~reflectance~~ data that is not captured in τ data. The two other panels (Fig. 7e,f) highlight the challenges with the choice of dimensionality. In the case of radiance versus τ, while there is a strong correlation in the occurrence frequency within the more reflective clouds, the structure in the MBL depth is much less clear. In the case of cloud fraction versus ECF, the occurrence frequency is much more poorly correlated and scattered, while the MBL depth shows less structure in either dimension.

We will use radiance ~~reflectance~~ versus ECF (Fig. 7a) in the remainder of this work. We are not advocating that the dimensional choices made are optimal. Instead, the results motivate the use of ~~a fresh look at available~~ satellite and reanalysis data~~, their joint distributions and statistical moments,~~ building from native resolution, pixel-scale, temporally instantaneous coincidences.

4.3 Regional similarity ~~differences~~ in MBL depth ~~and dMSE~~

The ~~occurrence~~ frequencies of AMSU FORs that contain stratocumulus and cumulus are listed in Table 1. The largest differences in the gradients between stratocumulus and cumulus are found in the NEP (Fig. 8a,e), while the smallest differences are found in the NEA (Fig. 8c,g). The MBL depth is several 10s of hPa shallower in stratocumulus (Fig. 8a-d) compared to cumulus (Fig. 8e-h) in all four regions~~. F~~ for almost every possible combination of radiance ~~reflectance~~ and ECF~~, it is encouraging that the MBL depth is shallower for stratocumulus than cumulus~~. We can conclude that the cloud amount and shortwave reflected radiation act independently of MBL depth. A small population of shallow MBL depths for ECF > 0.9 is found in cumulus (Fig. 8e-h) and is a consequence of a few ~~small sample size of~~ stratocumulus clouds that fail

to exhibit a large enough T_b signature to trigger liquid phase tests (e.g., Kahn et al., 2011; 2014). The two cloud regimes therefore should not be considered mutually exclusive of each other.

A significant increase in MBL depth with increasing radiance ~~reflectance~~ is found in cumulus with a stronger relationship ~~noted~~ in the NH compared to the SH (Fig. 8e-h) at a fixed value of ECF. This is partly a result of a deeper MBL in the SEP and SEA near the coastline (Fig. 4). The exception is that the NEP, SEP, and SEA ~~all~~ show a decrease for the most reflective clouds except for the NEA. Generally speaking the NEA is the largest outlier of the four regions for all radiance moments shown for MBL depth in Fig. 8 and is affected more by the midlatitudes than other regions. The MBL depth gradients have ~~demonstrate~~ an approximately ~~more~~ linear relationship with the standard deviation of radiance ~~reflectance~~ (Fig. 8i-l) unlike ~~than~~ the average radiance ~~reflectance~~ (Fig. 8e-h). The MBL is deepest for the largest values of the standard deviation at almost all values of ECF in all four regions. This suggests that the largest values of average radiance ~~reflectance~~ in Fig. 8e-h are uniform in spatial structure and have some of ~~among~~ the lowest standard deviations (Fig. 8e-h).

The radiance ~~reflectance~~ skewness is shown in Fig. 8m-p. There are several important features to describe. First, the MBL depth is shallower for normally distributed radiance ~~reflectance~~ and a sharp increase in MBL depth with increasing positive skewness is consistent with Figs. 3 and 4. Second, the change in MBL depth is somewhat greater for an identical increase in radiance ~~reflectance~~ skewness when compared to τ skewness (not shown). Third, the population of cumulus occurrences at low ECF for positive skewness > 1 are mostly absent in the τ data (not shown) but are very common in radiance ~~reflectance~~ data. We argue that this discrepancy has an important impact on the interpretation of the trade cumulus climatology. The gradient of MBL depth in the dimension of increasing positive skewness at low values of ECF is much greater in the radiance ~~reflectance~~ data where the highest data counts are found. We posit that the radiance ~~reflectance~~ data contain more ~~disorganized~~ subpixel cumulus missing in ~~than~~ the τ data. Fourth (not shown), ~~we remove~~ the AIRS cloud mask filter (Fig. 1b) is removed in order to retain all values of radiance ~~reflectance~~ (clear and cloudy) in the joint pdf. While the patterns of radiance ~~reflectance~~ skewness and MBL depth are not significantly altered when applying the cloud mask filter, many more counts with normally distributed radiances ~~reflectances~~ appear that indicates some leakage of weak clear-sky surface reflection. We conclude that there is a much bigger difference between the cloud mask-filtered radiance ~~reflectance~~ and τ, rather than between the filtered and non-filtered variants of radiance ~~reflectance~~, implying a robust interpretation. Fifth, the MBL depth contours change more rapidly with skewness of τ or radiance ~~reflectance~~ rather than with the mean value of τ or radiance ~~reflectance~~, consistent with the findings of Kawai and Teixeira (2010) where a tighter correlation with LWP skewness compared to average LWP was found.

Figure 9 shows that the dMSE in the SEP is positive in sign and largest in magnitude for larger values of ECF and normally distributed radiance ~~reflectance~~ (other regimes are similar and are not shown). In the case of radiance ~~reflectance~~ skewness, contours of constant dMSE track closely to the occurrence frequency through much of the joint pdfs, with a reduction of dMSE to values less than zero at a fixed value of ECF as positively skewed radiances ~~reflectance~~ increases. This behavior is similar to MBL depth (Fig. 8f) and suggests that instantaneous values of dMSE correlate~~d~~ well with small-scale ~~spatial~~

~~organization of~~ clouds~~s~~ variability. This is not inconsistent with LTS and dMSE correlating well ~~rather than the conventional wisdom that it best correlates~~ with larger-scale atmospheric thermodynamic structure on much longer time scales. Kawai and Teixeira (2012) showed that the skewness of LWP varies from +1 to +2 for cloud amounts of 90–100%, and up to +1.5 to +3.5 for cloud amounts < 30%. Furthermore, Kawai and Teixeira (2010) found that the highest correlations occur between LWP homogeneity, skewness and kurtosis to different measures of temperature and moisture differences from the surface to 850 hPa, rather than to values of EIS and LTS.

~~4.4 Vertical structure of RH~~

~~Figure 10 shows the three moments of AIRS RH in the cumulus-dominated SEP at four separate levels (700, 850, 925 and 1000 hPa). The driest air is observed at RH_{700}, while the moistest is observed at RH_{925} and RH_{1000}. Very similar magnitudes and gradients are observed for MERRA RH at all four levels and three statistical moments (Fig. A1). The largest magnitudes of RH correspond to the deepest MBLs (Fig. 8) and MERRA RH_{925} is as large as 95% (Fig. A1).~~

~~Despite known sensitivity limitations of infrared sounding in opaque clouds, and vertical smoothing due to the nature of satellite infrared weighting functions (see Appendix A), there exists a strong consistency between AIRS and MERRA RH in the cloudy subtropical MBL and lower free troposphere. This comparison demonstrates the value of both AIRS and MERRA RH and should lend confidence to the use of both data sets.~~

4.4 ~~4.5~~ Relating meteorology and microphysical processes

Nuijens et al. (2009) describe Rain in Cumulus over the Ocean (RICO) field campaign observations that illustrate fundamental physical relationships between cloud cover, wind speed and direction, the vertical structure of RH, and precipitation frequency and intensity within precipitating shallow trade cumulus. The observations can be grouped into three fairly distinct cumulus regimes: (i) low cloud fraction with little to no precipitation characterized by low values of u and a drier MBL; (ii) an increase in cloud fraction with some light precipitation characterized by low values of u and elevated RH between 800-1000 hPa; (iii) a further increase in cloud fraction with light precipitation and some isolated heavier events characterized by higher values of u and a large increase in RH between 650-900 hPa. A key observational difference among the three regimes is the variation of RH within the MBL (800-1000 hPa), and near the top of the MBL extending into the lower free troposphere (650-900 hPa). The width of these layers is similar to the AIRS 700 and 925 hPa temperature and specific humidity weighting functions. Even though the RICO observations do not fall within any of the four regions listed in Table 1, Medeiros and Nuijens (2016) show that the observational site is applicable to the trade regime as a whole across the globe. Thus our approach is to determine if similar relationships shown in Nuijens et al. (2009) exist in cumulus for the regions listed in Table 1.

Figure 10~~1~~1 shows the MODIS derived r_e for stratocumulus (Fig. 10~~1~~1a-d) and cumulus (Fig. 10~~1~~1e-p) that are limited to successful retrievals (no PCL pixels are included). There are several prominent features in the histograms. First, the stratocumulus r_e is about 11 to 12 μm throughout most of the pdf in all four regions. An exception is the increase of r_e by

several μm when average radiance ~~reflectance~~ and ECF are reduced (Fig. 10~~11~~a-d). While these particular MODIS pixels were successful, cloud horizontal inhomogeneity ~~may~~ causes larger r_e within this population of clouds because of the plane parallel homogeneous bias (Cho et al., 2015; Zhang et al., 2016). Cloud inhomogeneity may also lead to significant 3-D radiative transfer effects but these tend to cause both larger and smaller r_e in similar proportions (Zhang et al., 2012). Second, the NEA region (Fig. 10~~11~~g) is most dissimilar to the other three regions for average (Figs. 10~~11~~e-h), standard deviation (Fig. 10~~11~~i-l) and skewness (Fig. 10~~11~~m-p). Third, ~~the~~ r_e is largest along the axis of maximum counts with values upwards of 16 to 20 μm in the SEP, 15-18 μm in the SEA, and 14–17 μm in the NEP. The largest values in the NEA are confined to the most skewed radiances ~~reflectances~~ unlike the other three regions. Fourth, in the cleaner SH, the values of r_e appear to be more tightly coupled to cloud microphysical processes that respond to changing wind speed and a deepening MBL ~~(see Section 4.6)~~.

One general interpretation of the larger r_e in cumulus (Fig. 10e-h) when contrasted to stratocumulus (Fig. 10a-d) is that it is caused by ~~relates to the~~ increased inhomogeneity of cumulus (Zhang et al., 2012~~, 2016~~), retrieval failures and partly cloudy pixels (Cho et al., 2015), and view angle biases (e.g., Liang et al., 2015) that are further coupled together with other factors at play ~~in numerous and complex ways~~ (Zhang et al., 2016 ~~Cho et al., 2015~~). The aforementioned issues may still impact a successful r_e retrieval. ~~As these particular MODIS pixels are limited to successful retrievals only,~~ However, we offer evidence that the increase in r_e is also ~~entirely~~ consistent with environmental variability that in turn is ~~furthermore~~ consistent with droplet growth and precipitation. The contours of r_e correspond very closely to the magnitude of the u-component of wind speed at 925 hPa (u_{925}) (see Fig. 12 ~~Section 4.6~~) and other levels in the MBL (not shown), suggesting a link between cloud droplet growth, light rain, and dynamical variability. The somewhat larger r_e in the SH is consistent with droplet growth in a cleaner environment (Suzuki et al., 2010a,b). Successful retrievals with pixels that have increased subpixel horizontal inhomogeneity may be more frequently precipitating, either because of larger r_e in the cloud, or because the plane parallel homogeneous bias is larger in precipitating clouds. ~~could produce larger r_e (Cho et al., 2015), and furthermore could be correlated with increased precipitation frequency. Zhang et al. (2016) show primarily large r_e in scenes with inhomogeneity, although a smaller fraction of clouds have smaller r_e~~.

To determine if the elevated r_e along the axis of maximum counts is associated with increased precipitation frequency, ~~we use~~ collocated matchups of the CloudSat precipitation rate are used to determine which AMSU FOVs contain occurrences of precipitation. Figure 11~~12~~ shows results for the SEP region. The radiance ~~reflectance~~ skewness for the full AIRS/AMSU/MODIS swath in Fig. 10~~11~~n is restricted to the CloudSat ground track in Fig. 11~~12~~a. The counts are reduced by a factor ~~in excess~~ of ~30 as expected. There are some subtle changes in the r_e distribution showing an increase of 2-3 μm with increasing skewness at a fixed value of ECF. Figure 11~~12~~b shows the proportion of the pdf that contains at a minimum the natural log(2) counts of precipitation occurrence within each bin. About 20-50% of the AMSU FOVs are precipitating according to CloudSat within the pdf of Fig. 11~~12~~a. The precipitation frequency is consistent with Rapp et al. (2013) where up to 40% of clouds precipitate in the cumulus regime. Little to no precipitation occurs outside of the central portion of the pdf in Fig. 11~~12~~a. The highly skewed cumulus with ECF<0.2 appear to be exhibiting large r_e biases due to visible radiance

~~reflectance~~ inhomogeneity (Cho et al., 2015; Zhang et al., 2016). We also point out that the population of clouds detected by CloudSat that have ECF>0.95 (Fig. 11~~12~~b) are associated with very little precipitation and is consistent with the spatial distributions described by Rapp et al. (2013).

~~4.6 Variations of u and ω~~

Figure 12~~13~~ shows $\theta_{e,700}$, u_{925}, ω_{700}, and ω_{925}. The θ_{700} (not shown) is nearly identical among all regions with θ_{700}=314 K ± 1 K. Thus, the structure in $\theta_{e,700}$ (Fig. 12~~13~~a-d) ~~and RH_{700}~~ is driven by variations in specific humidity. For a fixed value of ECF, the clouds with the lowest and highest values of radiance ~~reflectance~~ are associated with moistening of the lower free troposphere. Using climatological averages, Myers and Norris (2015) show that shortwave observations from CERES, cloud fraction estimates from ISCCP and CALIPSO, and RH_{700} and ω_{700} from ERA-Interim reflect aspects of Fig. 12~~13~~ and, namely, that more reflected shortwave is associated with increased cloud fraction and decreased ω_{700}.

The highest values of $\theta_{e,925}$ (not shown) occur along the axis of highest counts while reductions in $\theta_{e,925}$ occur for the least and most reflective clouds at a fixed value of ECF. This is the case for the NEP, SEP, and SEA, but the NEA is an outlier and shows a constant increase as seen with RH and MBL depth. Unlike 700 hPa, θ_{925} is more variable (not shown) between the four regions but is generally 2 K or less.

The u_{925} is largest (Fig. 12~~13~~e-h) when the pdf has the largest counts and very closely resembles r_e in Fig. 10~~11~~e-h. The subtle differences in the contours in Fig. 10~~11~~e-h and Fig. 12~~13~~e-h align very well, suggesting a tight correlation between the two parameters. The magnitude of u_{925} is larger than u_{700} (not shown) consistent with RICO (Nuijens and Stevens, 2009). The ω_{700} fields (Fig. 12~~13~~i-l) exhibit minimal correspondence with average radiance ~~reflectance~~ and ECF in the NH regimes with a weak correspondence in the average radiance ~~reflectance~~ in the SH regions. The ω_{925} fields (Fig. 12~~13~~m-p) show larger gradients in all four regions. The ω_{925} decreases with increasing radiance ~~reflectance~~ in all regions similar to that shown in Myers and Norris (2015), with a slightly noisier pattern in ω_{925} observed in the NH regimes. The decrease of ω_{925} with increasing radiance ~~reflectance~~ is consistent with a deeper MBL (Fig. 8e-h) and larger τ. Where u_{925} (Fig. 12~~13~~e-h) increases, ω_{925} (Fig. 12~~13~~m-p) decreases and RH_{925} increases (not shown). The largest values of r_e (Fig. 10~~11~~e-h) also correspond to the above tendencies, consistent with the concept of more frequent precipitating clouds within a windier and deeper MBL (Nuijens and Stevens, 2012).

The joint pdfs imply simultaneous increases in $\theta_{e,700}$, $\theta_{e,925}$ (and by extension RH_{700} and RH_{925}), u_{925}, and ECF in three of the four regions investigated (NEP, SEP, and SEA) with a particularly strong relationship between u_{925} and r_e. The NEA is somewhat of an outlier although this is based on one seasons' worth of data during 2009. There is much variability across the trade cumulus regime as it is ~~should~~ not ~~be treated as~~ a single homogeneous entity. ~~The satellite and reanalysis observations are able to quantify aspects of the non-uniqueness between free tropospheric and MBL humidity, cloud coverage, wind speed, subsidence, and precipitation frequency.~~

5 Summary and Conclusions

The global-scale relationships of cloud fraction and spatial variability ~~organization~~ to thermodynamic and dynamic properties of the atmosphere remain poorly understood. The NASA A-train (Stephens et al., 2002) provides a wealth of remote sensing data about the microphysics and thermodynamics of the cloudy MBL. The Modern Era Retrospective-Analysis for Research and Applications (MERRA; Rienecker et al., 2011) offers a complementary set of thermodynamic and dynamic variables that helps establish context for coincident remote sensing observations. The synergy between satellite and reanalysis data at the native spatial and temporal resolutions available has not been fully exploited to date. We describe an ~~a nov~~el approach that leverages coincident reanalysis and remote sensing data at the native resolution of the observations. The spatial variability ~~organization~~ of clouds, and the relationship to thermodynamic and dynamic state variables, is thus inferred using the finest temporal and spatial resolutions available.

Four subtropical oceanic regions that capture transitions from ~~organized closed-cell~~ stratocumulus to ~~disorganized open-cell~~ trade cumulus are investigated ~~(Klein and Hartmann, 1993; Muhlbauer et al., 2014)~~. We define two regimes based exclusively on *liquid* and *unknown* cloud thermodynamic phase detections with the AIRS instrument, and generically refer to them as *stratocumulus* and *cumulus* regimes, respectively. The mean, standard deviation, and skewness of MODIS and AIRS FOV cloud properties and visible radiances ~~reflectances~~ are calculated for each AIRS and MERRA temperature and humidity observation.

As with previous findings, coastal stratocumulus radiances ~~reflectances~~ are approximately normally distributed while the radiances ~~reflectances~~ are positively skewed away from the coast where disorganized cumulus dominates. The radiance ~~reflectance~~ skewness closely aligns to the magnitude of AIRS effective cloud fraction (ECF) in cumulus with less correspondence in stratocumulus. Strong (poor) spatial correspondence between radiance ~~reflectance~~ skewness and AIRS ECF (MODIS cloud fraction) was found suggesting infrared-based ECF is a ~~an unappreciated and~~ potentially valuable diagnostic for MBL cloud characterization. The mean MBL depth derived from AIRS (Martins et al., 2010) shows a characteristic transition from shallow MBLs (920–970 hPa) near the coast to deeper MBLs (830–880 hPa) away from the coast and is a well-observed feature of the stratocumulus to cumulus transition (e.g., Teixeira et al., 2011). ~~RH at 700 hPa in the SH is lower than the NH while the NEA is the moistest of the four regions and SEP the driest.~~ The AIRS-derived moist static energy differences (dMSE) between 700 and 1000 hPa agree very well with ERA-Interim (Kubar et al., 2012). We find that the radiance ~~reflectance~~ skewness is strongly related to ~~cloud organization and~~ the magnitude of dMSE as previously found by Kawai and Teixeira (2012). ~~For almost every possible combination of reflectance and ECF, it is encouraging that t~~ The MBL depth is shallower for stratocumulus than cumulus.

The change in MBL depth is somewhat greater for an identical increase in radiance ~~reflectance~~ skewness when compared to τ skewness. The population of cumulus occurrences at low ECF for positive skewness > 1 are mostly absent in the τ data but are very common in radiance ~~reflectance~~ data. This highlights the importance of understanding the sampling from derived

Level 2 products compared to Level 1 radiances ~~and reflectances~~ that may capture a fuller range of the geophysical state in different cloud regimes.

~~The lowest RH is observed at 700 and 850 hPa above stratocumulus, while the highest is observed at 925 hPa in proximity to shallow cumulus. The difference between MERRA and AIRS RH at 925 hPa increases as reflectance or τ increases and reaffirms the well-known sampling bias of satellite infrared sounding within the cloudy MBL (Fetzer et al., 2006). While AIRS is unable to sample the moistest filaments within clouds that are opaque to infrared radiation, AIRS is able to replicate relative changes in RH exhibited by MERRA. The strong consistency between AIRS and MERRA RH in the cloudy subtropical MBL and lower free troposphere demonstrates the value of both AIRS and MERRA RH as reference data sets.~~

The r_e in stratocumulus is about 11 to 12 μm for most values of radiance ~~reflectance~~ and ECF in all four regions of study. For cumulus, r_e ranges anywhere from 12 to 20 μm, with larger r_e for increasing positive skewness especially when ECF is small. The values of r_e ~~are more~~ appear to be tightly coupled to cloud microphysical processes that respond to changing MBL wind speed and a deepening MBL. We argue that for these successful MODIS retrievals, the increase in r_e is consistent with increased droplet growth and hence precipitation occurrence. This may be caused by larger r_e in the cloud itself or that precipitating clouds are associated with an increased subpixel inhomogeneity that leads to the plane parallel homogeneous bias; this topic warrants further investigation. In the SEP region, ~~we confirm that~~ the elevated values of r_e that correspond with the increased u_{925} are more frequently ~~in fact~~ precipitating ~~much more frequently~~ according to CloudSat. ~~Clouds are non-precipitating if they are highly skewed with low values of ECF. This result is consistent with the idea that 3-D radiative effects, cloud inhomogeneity and algorithm assumptions break down in highly inhomogeneous shallow cumulus (Cho et al., 2015; Zhang et al., 2016).~~

The Rain in Cumulus over the Ocean (RICO) observations provide an important multi-parameter testing benchmark (Nuijens et al., 2009). These results are generalized into three types of shallow precipitating cumulus regimes observed during RICO. The joint pdfs imply simultaneous increases in $\theta_{e,700}$, $\theta_{e,925}$, u_{925}, and ECF in three of the four regions investigated (NEP, SEP, and SEA) with a strong correspondence between u_{925} and r_e. The NEA less clearly follows these behaviors and is an outlier, although this is based on one seasons' worth of data during 2009. ~~The variability among the different regions of study emphasizes the non-uniqueness among changes in free tropospheric humidity, cloud coverage, wind speed, and subsidence. Our results are consistent with Nuijens and Stevens (2009) and may offer additional insight into the global context of the structure of the subtropical cumulus-dominated MBL when a larger observational record is examined.~~

Future work will expand to other cloud regimes, additional data sets, and multiple years of data. A similar approach with numerical model output should also be attempted using temporal snapshots of similar geophysical fields. We expect that this approach will be especially useful for linking cloud microphysics together with the thermodynamic and dynamic state of the atmosphere at the process scale.

~~**Appendix A**~~

~~The differences between MERRA and AIRS RH_{925} are greater as reflectance increases and helps quantify the magnitude of the well-known clear-sky sampling bias of atmospheric infrared sounding (Fetzer et al., 2006) within the cloudy MBL. These results reaffirm the notion that AIRS is unable to sample the moistest filaments of the MBL that reside within clouds that are opaque to infrared radiation. Given this tendency, however, AIRS is still able to replicate the changes in RH exhibited by MERRA with respect to the magnitude of reflectance. Furthermore, when the clouds are generally broken or semi-transparent, the magnitude of AIRS and MERRA RH_{925} is more similar. Lastly, AIRS RH_{1000} is about 75-80% (Fig. 10) and about 80-85% for MERRA (Fig. A1) and are both near typical values for the low-latitude oceans (Richter and Xie, 2008). Uniform values of RH_{1000} are found for all combinations of reflectance and ECF.~~

Acknowledgments

Part of this research was carried out at the Jet Propulsion Laboratory (JPL), California Institute of Technology, under a contract with the National Aeronautics and Space Administration. GM and BHK were partially supported by an R&TD project at JPL. BHK was partially supported by the AIRS project at JPL and by the NASA Science of Terra and Aqua program under grant NNN13D455T. BHK, QY, and MMS were partially supported by NASA's Making Earth Science Data Records for Use in Research Environments (MEaSUREs) program. The authors thank two reviewers for comments and suggestions that led to an improved version of this manuscript. The AIRS version 6 data sets were processed by and obtained from the Goddard Earth Services Data and Information Services Center (http://daac.gsfc.nasa.gov/). The MODIS collection 6 data sets were processed by and obtained from the Level 1 and Atmosphere and Archive Distribution System (http://ladsweb.nascom.nasa.gov). The MERRA data sets were processed by and obtained from the NASA Goddard's Global Modeling and Assimilation Office (GMAO). CloudSat data were obtained through the CloudSat Data Processing Center (http://www.cloudsat.cira.colostate.edu/). The data and code used in this investigation is available upon request from the lead author

References

~~Atkinson, B. W., and Zhang, J. W.: Mesoscale shallow convection in the atmosphere, Rev. Geophys., 34, 403-431, 1996.~~

Aumann, H. H., Broberg, S., Elliott, D., Gaiser, S., and Gregorich, D.: Three years of Atmospheric Infrared Sounder radiometric calibration validation using sea surface temperatures, J. Geophys. Res., 111, D16S90, doi:10.1029/2005JD006822, 2006.

Bony, S. and Dufresne, J. L.: Marine boundary layer clouds at the heart of tropical cloud feedback uncertainties in climate models, Geophys. Res. Lett., 32, L20806, doi:10.1029/2005GL023851, 2005.

Bretherton, C. S., Wood, R., George, R. C., Leon, D., Allen, G., and Zheng, X.: Southeast Pacific stratocumulus clouds, precipitation and boundary layer structure sampled along 20°S during VOCALS-REx, Atmos. Chem. Phys., 10, 10639–10654, 2010.

Bretherton, C. S., Blossey, P. N., and Jones, C. R.: Mechanisms of marine low cloud sensitivity to idealized climate perturbations: A single-LES exploration extending the CGILS cases, J. Adv. Model. Earth Sys., 5, 316–337, doi:10.1002/jame.20019, 2013.

~~Brient, F., and Bony, S.: Interpretation of the positive low-cloud feedback predicted by a climate model under global warming, Clim. Dyn., 40, 2415–2431, 2013.~~

Brueck, M., Nuijens, L., and Stevens, B.: On the seasonal and synoptic time-scale variability of the North Atlantic trade wind region and its low-level clouds, J. Atmos. Sci., 72, 1428–1446, 2015.

Cahalan, R. F., Ridgway, W., Wiscombe, W. J., and Bell, T. L.: The albedo of fractal stratocumulus clouds, Mon. Wea. Rev., 51, 2434–2455, 1994.

Caldwell, P. M., Zhang, Y., and Klein, S. A.: CMIP3 subtropical stratocumulus cloud feedback interpreted through a mixed-layer model, J. Climate, 26, 1607–1625, 2013.

Chahine, M. T., Pagano, T. S., Aumann, H. H., and Coauthors: The Atmospheric Infrared Sounder (AIRS): Improving weather forecasting and providing new insights into climate, B. Am. Meteor. Soc., 87, 911–926, doi:10.1175/BAMS-87-7-911, 2006.

Chan, K. M., and Wood, R.: The seasonal cycle of planetary boundary layer depth determined using COSMIC radio occultation data, J. Geophys. Res. Atmos., 118, 12,422–12,434, doi:10.1002/2013JD020147, 2013.

~~Christensen, M. W., Carrio, G. G., Stephens, G. L., and Cotton, W. R.: Radiative impacts of free tropospheric clouds on the properties of marine stratocumulus, J. Atmos. Sci., 70, 3102–3118, 2013.~~

Cho, H.-M., et al.: Frequency and causes of failed MODIS cloud property retrievals for liquid phase clouds over global oceans, J. Geophys. Res. Atmos., 120, 4132–4154, 2015, doi:10.1002/ 2015JD023161.

Chung, D., Matheou, G., and Teixeira, J.: Steady-state large-eddy simulations to study the stratocumulus to shallow cumulus cloud transition, J. Atmos. Sci., 69, 3264–3276, doi:10.1175/JAS-D-11-0256.1, 2012.

Clement, A. C., Burgman, R., and Norris, J. R.: Observational and model evidence for positive low-level cloud feedback, Science, 325, 460–464, doi:10.1126/science.1171255, 2009.

Dal Gesso, S., Siebesma, A. P., and de Roode, S. R.: Evaluation of low-cloud climate feedback through single-column model equilibrium states, Q. J. Royal Met. Soc., 141, 819–832, doi:10.1002/qj.2398, 2015.

Fasullo, J. T., and Trenberth, K. E.: A less cloudy future: The role of subtropical subsidence in climate sensitivity, Science, 338, 792–795, doi:10.1126/science.1227465, 2012.

Fetzer, E. J., Lambrigtsen, B. H., Eldering, A., Aumann, H. H., and Chahine, M. T.: Biases in total precipitable water vapor climatologies from Atmospheric Infrared Sounder and Advanced Microwave Scanning Radiometer, J. Geophys. Res., 111, D09S16, doi:10.1029/2005JD006598, 2006.

Gautier, C., Shiren, Y., and Hofstadter, M. D.: AIRS/Vis Near IR instrument, IEEE Trans. Geosci. Remote Sens., 41, 330–342, 2003.

Ghate, V. P., Miller, M. A., and Zhu, P.: Differences between nonprecipitating tropical and trade wind marine shallow cumuli, Mon. Wea. Rev., 144, 681–701, 2016.

IPCC: Climate Change 2013: The Physical Science Basis. Contribution of Working Group I to the Fifth Assessment Report of the Intergovernmental Panel on Climate Change, edited by T. F. Stocker, et al., 1535 pp., Cambridge Univ. Press, Cambridge, U. K., and New York, doi:10.1017/CBO9781107415324, 2013.

Jin, H., and Nasiri, S. L.: Evaluation of AIRS cloud-thermodynamic-phase determination with CALIPSO, J. Appl. Meteor. Climatol., 53, 1012–1027, 2014.

Kahn, B. H.,. Nasiri, S. L, Schreier, M. M., and Baum, B. A.: Impacts of subpixel cloud heterogeneity on infrared thermodynamic phase assessment, J. Geophys. Res., 116, D20201, doi:10.1029/2011JD015774, 2011.

Kahn, B. H., Irion, F. W., Dang, V. T., and Coauthors: The Atmospheric Infrared Sounder Version 6 cloud products, Atmos. Chem. Phys., 14, 399–426, 2014.

Kalmus, P., Wong, S., and Teixeira, J.: The Pacific subtropical cloud transition: A MAGIC assessment of AIRS and ECMWF thermodynamic structure, IEEE Geosci. Remote Sens. Lett., 12, 1586–1590, doi:10.1109/LGRS.2015.2413771, 2015.

Karlsson, J., Svensson, G., Cardoso, S., Teixeira, J., and Paradise, S.: Subtropical cloud-regime transitions: boundary layer depth and cloud-top height evolution in models and observations, J. Appl. Meteor. Climatol., 49, 1845–1858, 2010.

Kawai, H., and Teixeira, J.: Probability density functions of liquid water path and cloud amount of marine boundary layer clouds: Geographical and seasonal variations and controlling meteorological factors, J. Climate, 23, 2079–2092, 2010.

Kawai, H., and Teixeira, J.: Probability density functions of liquid water path and total water content of marine boundary layer clouds: Implications for cloud parameterization, J. Climate, 25, 2162–2177, 2012.

Klein, S. A., and Hartmann, D. L.: The seasonal cycle of low stratiform clouds, J. Climate, 6, 1587–1606, 1993.

Kubar, T. L., Waliser, D. E., Li, J.-L., and Jiang, X.: On the annual cycle, variability, and correlations of oceanic low-topped clouds with large-scale circulation using Aqua MODIS and ERA-Interim, J. Climate, 25, 6152–6174, 2012.

Kubar, T. L., Stephens, G. L., Lebsock, M., Larson, V. E., and Bogenschutz, P. A.: Regional assessments of low clouds against large-scale stability in CAM5 and CAM-CLUBB using MODIS and ERA-Interim reanalysis data, J. Climate, 28, 1685–1706, 2015.

L'Ecuyer, T. S., and Stephens, G. L.: An estimation-based precipitation retrieval algorithm for attenuating radars. *J. Appl. Meteor.*, **41**, 272–285, 2002, doi:10.1175/1520-0450(2002)041<0272:AEBPRA>2.0.CO;2.

Lau, K. M., and Kim, K.-M.: Robust Hadley circulation changes and increasing global dryness due to CO2 warming from CMIP5 model projections, Proc. Natl. Acad. Sci., 112, 3630–3635, 2015.

Liang, L., Di Girolamo, L., and Sun, W: Bias in MODIS cloud drop effective radius for oceanic water clouds as deduced from optical thickness variability across scattering angles, J. Geophys. Res. Atmos., 120, 7661–7681, 2015, doi:10.1002/2015JD023256.

Maddy, E. S., and Barnet, C. D.: Vertical resolution estimates in Version 5 of AIRS operational retrievals, IEEE Trans. Geosci. Remote Sens., 46, 2375–2384, 2008.

Martins, J. P. A., Teixeira, J., Soares, P. M. M., Miranda, P. M. A., Kahn, B. H., Dang, V. T., Irion, F. W., Fetzer, E. J., and Fishbein, E.: Infrared sounding of the trade-wind boundary layer: AIRS and the RICO experiment, Geophys. Res. Lett., 37, L24806, doi:10.1029/2010GL045902, 2010.

Medeiros, B. P., and Stevens, B.: Revealing differences in GCM representations of low clouds, Clim. Dyn., 36, 385–399, 2011.

Medeiros, B. P., and Nuijens, L.: Clouds at Barbados are representative of clouds across the trade wind regions in observations and climate models, Proc. Natl. Acad. Sci., 113(22):E3062-70, 2016, doi: 10.1073/pnas.1521494113.

Muhlbauer, A., McCoy, I. L., and Wood, R.: Climatology of stratocumulus cloud morphologies: microphysical properties and radiative effects, Atmos. Chem. Phys., 14, 6695–6716, 2014.

Myers, T. A., and Norris, J. R.: On the relationship between subtropical clouds and meteorology in observations and CMIP3 and CMIP5 models, J. Climate, 28, 2945–2967, 2015.

Nam, C., Bony, S., Dufresne, J.-L., and Chepfer, H.: The 'too few, too bright' tropical low-cloud problem in CMIP5 models, Geophys. Res. Lett., 39, L21801, 2012, doi:10.1029/2012GL053421.

~~Nasiri, S. L., Dang, V. T., Kahn, B. H., Fetzer, E. J., Manning, E. M., Schreier, M. M., and Frey, R. A.: Comparing MODIS and AIRS infrared-based cloud retrievals, J. Appl. Meteorol. Climatol., 50, 1057–1072, doi:10.1175/2010JAMC2603.1, 2011.~~

Nuijens, L., B. Stevens, and A. P. Siebesma: The environment of precipitating shallow cumulus convection, J. Atmos. Sci., 66, 1962–1979, 2009.

Nuijens, L., and Stevens, B.: The influence of wind speed on shallow marine cumulus convection, J. Atmos. Sci., 69, 168–184, 2012.

Oreopoulos, L., and Cahalan, R. F.: Cloud inhomogeneity from MODIS, J. Climate, 18, 5110–5124, 2005.

~~Platnick, S., King, M. D., Ackerman, S. A., Menzel, W. P., Baum, B. A., and Frey, R. A.: The MODIS cloud products: Algorithms and examples from Terra, IEEE Trans. Geosci, Remote Sens. 41, 459–473, 2003.~~

Platnick, S., Meyer, K. G., King, M. D., and Coauthors: The MODIS cloud optical and microphysical products: Collection 6 updates and examples from Terra and Aqua, IEEE Trans. Geosci. Remote Sens., 55, 502–525, 2017.

Rapp, A. D., Lebsock, M., and T. L'Ecuyer, T.: Low cloud precipitation climatology in the southeastern Pacific marine stratocumulus region using CloudSat, Environ. Res. Lett., 8, 2013, doi:10.1088/1748-9326/8/1/014027.

Richter, I., and Xie, S.-P.: Muted precipitation increase in global warming simulations: A surface evaporation perspective, J. Geophys. Res., 113, D24118, doi:10.1029/2008JD010561, 2008.

Rieck, M., Nuijens, L., and Stevens, B.: Marine boundary layer cloud feedbacks in a constant relative humidity atmosphere, J. Atmos. Sci., 69, 2538–2550, 2012.

Rienecker, M. M., Suarez, M. J., Gelaro, R., and Coauthors: MERRA: NASA's Modern-Era Retrospective Analysis for Research and Applications. J. Climate, 24, 3624-3648, doi:10.1175/JCLI-D-11-00015.1, 2011.

Rossow, W. B. and Schiffer, R. A.: Advances in Understanding Clouds from ISCCP, B. Am. Meteorol. Soc., 72, 2–20, 1999.

~~Sandu, I., and Stevens, B.: On the factors modulating the stratocumulus to cumulus transitions, J. Atmos. Sci., 68, 1865–1881, 2011.~~

Schreier, M. M., Kahn, B. H., Eldering, A., Elliott, D. A., Fishbein, E., Irion, F. W., and Pagano, T. S.: Radiance comparisons of MODIS and AIRS using spatial response information, J. Atmos. Oceanic Technol., 27, 1331–1342, doi:10.1175/2010JTECHA1424.1, 2010.

Sherwood, S. C., Ingram, W., Tsushima, Y., Satoh, M., Roberts, M., Vidale, P. L., and O'Gorman, P. A.: Relative humidity changes in a warmer climate, J. Geophys. Res., 115, D09104, doi:10.1029/2009JD012585, 2010.

Stephens, G. L., Vane, D. G., Boain, R. J., and Coauthors: The CloudSat mission and the A-train, Bull. Amer. Meteor. Soc., 83, 1771–1790, 2002.

Stephens, G. L.: Cloud feedbacks in the climate system: A critical review, J. Climate, 18, 237–273, 2005.

Suselj, K., Teixeira, J., and Chung, D.: A unified model for moist convective boundary layers based on a stochastic eddy-diffusivity/mass-flux parameterization, J. Atmos. Sci., 70, 1929–1953, 2013.

Suzuki, K., Nakajima, T., Nakajima, T. Y., and Khain, A. P.: A study of microphysical mechanisms for correlation patterns between droplet radius and optical thickness of warm clouds with a spectral bin microphysics cloud model, J. Atmos. Sci., 67, 1126–1141, 2010a.

Suzuki, K., Nakajima, T., Nakajima, T. Y., and Stephens, G. L.: Effect of the droplet activation process on microphysical properties of warm clouds, Environ. Res. Lett., 5, 1–6, 2010b, doi:10.1088/1748-9326/5/2/024012.

Teixeira, J., Cardoso, S., Bonazzola, M., and Coauthors: Tropical and subtropical cloud transitions in weather and climate prediction models: The GCSS/WGNE Pacific cross-section intercomparison (GPCI), J. Climate, 24, 5223–5256, 2011.

~~Tian, B., Fetzer, E. J., Kahn, B. H., Teixeira, J., Manning, E., and Hearty, T.: Evaluating CMIP5 Models using AIRS Tropospheric Air Temperature and Specific Humidity Climatology, J. Geophys. Res. Atmos., 118, 114–134, doi:10.1029/2012JD018607, 2013.~~

~~Vergados, P., Mannucci, A. J., Ao, C. O., Jiang, J. H., and Su, H.: On the comparisons of tropical relative humidity in the lower and middle troposphere among COSMIC radio occultations and MERRA and ECMWF data sets, Atmos. Meas. Tech., 8, 1789–1797, 2015.~~

von Engeln, A., Teixeira, J., and Beyerle, G.: Impact of thin water vapor layers on CHAMP radio occultation measurements, Radio Sci., 42, RS2010, doi:10.1029/2005RS003379, 2007.

Weber, T., Quaas, J., and Räisänen, P.: Evaluation of the statistical cloud scheme in the ECHAM5 model using satellite data. Q.J.R. Meteorol. Soc., 137, 2079–2091. doi: 10.1002/qj.887, 2011.

Wood, R., and Bretherton, C. S.: Boundary layer depth, entrainment and decoupling in the cloud-capped subtropical and tropical marine boundary layer, J. Clim., 17, 3576–3588, 2004.

Wood, R., and Hartmann, D. L.: Spatial variability of liquid water path in marine boundary layer clouds: The importance of mesoscale cellular convection. J. Climate, 19, 1748–1764, 2006.

Wood, R., and Field, P. R.: The Distribution of Cloud Horizontal Sizes. J. Climate, 24, 4800–4816. doi: http://dx.doi.org/10.1175/2011JCLI4056.1, 2011.

Wood, R.: Stratocumulus Clouds. Mon. Wea. Rev., 140, 2373–2423. doi: http://dx.doi.org/10.1175/MWR-D-11-00121.1, 2012.

Yue, Q., Kahn, B. H., Fetzer, E. J., and Teixeira, J.: Relationship between oceanic boundary layer clouds and lower tropospheric stability observed by AIRS, CloudSat, and CALIOP, J. Geophys. Res., 116, D18212, doi:10.1029/2011JD016136, 2011.

Yue, Q., Kahn, B. H., Xiao, H., Schreier, M. M., Fetzer, E. J., Teixeira, J., and Suselj, K.: Transitions of cloud-topped marine boundary layers characterized by AIRS, MODIS, and a large eddy simulation model, J. Geophys. Res. Atmos., 118, 8598–8611, doi:10.1002/jgrd.50676, 2013.

Yue, Q., Kahn, B. H., Fetzer, E. J., Wong, S., Frey, R., and Meyer, K. G.: On the response of MODIS cloud coverage to global mean surface air temperature, J. Geophys. Res. Atmos., 121, doi:10.1002/2016JD025174, 2016.

Zelinka, M. D., Klein, S. A., and Hartmann, D. L.: Computing and partitioning cloud feedbacks using cloud property histograms. Part II: Attribution to changes in cloud amount, altitude, and optical depth, J. Climate, 25, 3736–3754, 2012.

Zhang, Z., Ackerman, A. S., Feingold, G., Platnick, S., Pincus, R., and Xue, H.: Effects of cloud horizontal inhomogeneity and drizzle on remote sensing of cloud droplet effective radius: Case studies based on large-eddy simulations, J. Geophys. Res., 117, D19208, doi:10.1029/2012JD017655, 2012.

Zhang, Z., Werner, F., Cho, H.-M., Wind, G., Platnick, S., Ackerman, A. S., Di Girolamo, L., Marshak, A., and Meyer, K.: A framework based on 2-D Taylor expansion for quantifying the impacts of subpixel reflectance variance and covariance on cloud optical thickness and effective radius retrievals based on the bispectral method, J. Geophys. Res. Atmos., 121, 7007–7025, 2016, doi:10.1002/2016JD024837.

Zhao, G., Di Girolamo, L., Diner, D. J., Bruegge, C., J., Mueller, K. J., and Wu, D. L.: Regional changes in Earth's color and texture as observed from space over a 15-year period, IEEE Trans. Geosci. Remote Sens., 54, 4240–4249, 2016.

Zhu, P., and Zuidema, P.: On the use of PDF schemes to parameterize sub-grid clouds, Geophys. Res. Lett., 36, L05807, doi:10.1029/2008GL036817, 2009.

Region	Abbrev	Season	Location	% Sc	% Cu	% Other	% Clr	Counts
Northeast Pacific Ocean	NEP	JJA	15°N–35°N 110°W–150°W	23.3	64.8	10.7	1.3	186133
Northeast Atlantic Ocean	NEA	JJA	15°N–35°N 10°W–50°W	8.1	72.0	18.0	1.9	183798
Southeast Pacific Ocean	SEP	SON	5°S–25°S 70°W–110°W	25.5	69.6	3.9	1.0	184208
Southeast Atlantic Ocean	SEA	SON	5°S–25°S 25°W–15°E	31.8	62.1	4.4	1.7	180668

Table 1: The four regions investigated in this study are greatly expanded in area from Klein and Hartmann (1993). The four ~~right~~ columns with percentages and total counts are defined at the AIRS/AMSU field of regard (FOR) spatial scale. The three cloudy categories indicate whether clouds of that type occur with any frequency within the AIRS/AMSU FOR. Clear is defined over the entire AIRS/AMSU FOR and are therefore very infrequent.

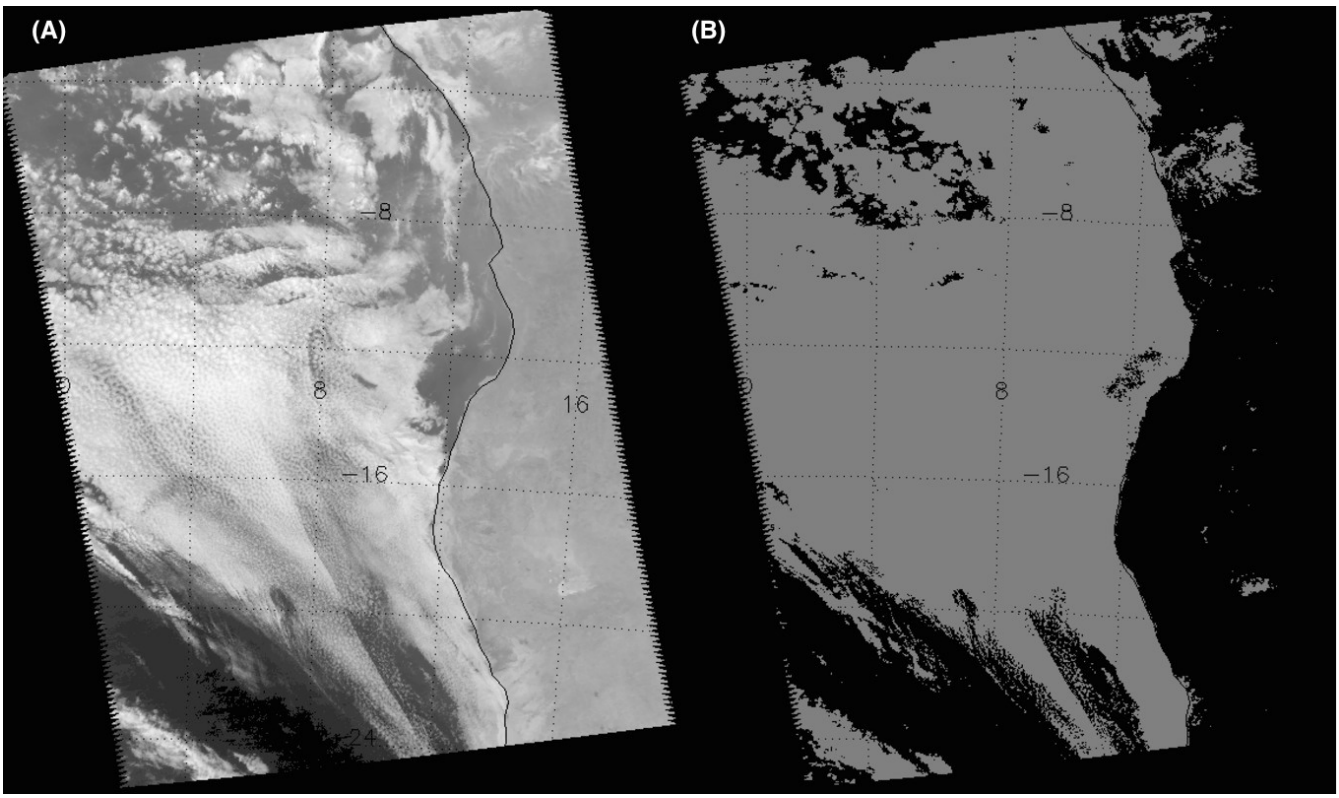

Figure 1. AIRS version 5 visible channel 4 radiance ~~reflectance~~ (0.49–0.94 μm) at a nadir spatial resolution of 2.28 km (left), and AIRS cloud mask (binary clear and cloudy) determined from visible channel thresholds (right). See *Gautier et al.* [2003] for more details.

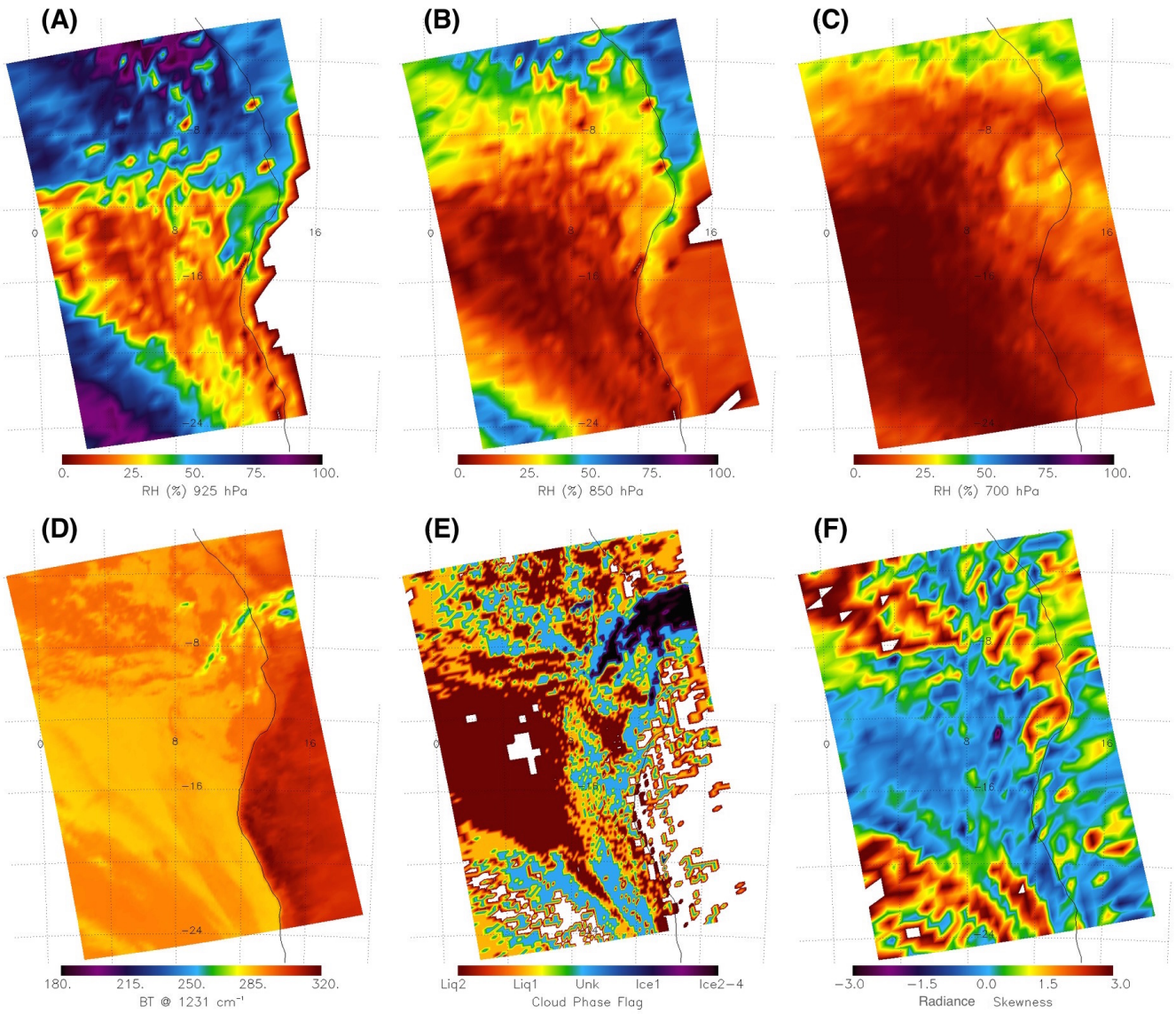

Figure 2. AIRS (a) RH_{925} (%), (b) RH_{850} (%), (c) RH_{700} (%), (d) 1231 cm^{-1} T_b (K), (e) cloud thermodynamic phase, and (f) radiance ~~reflectance~~ skewness from visible channel 4. The granule is identical to the one shown in Fig. 1.

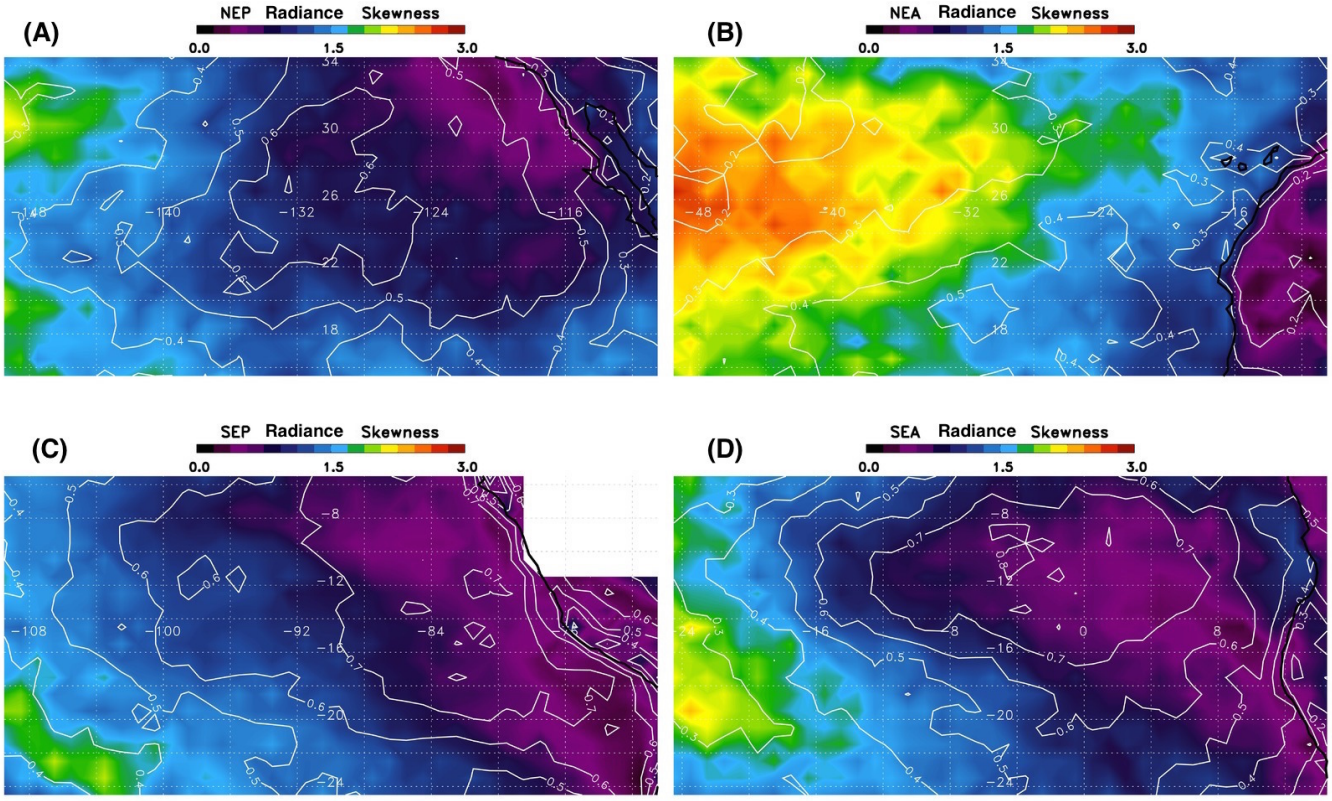

Figure 3. Radiance ~~Reflectance~~ **skewness for regions listed in Table 1: (a) NEP, (b) NEA, (c), SEP, and (d) SEA. The AIRS ECF is overlaid as white contours.**

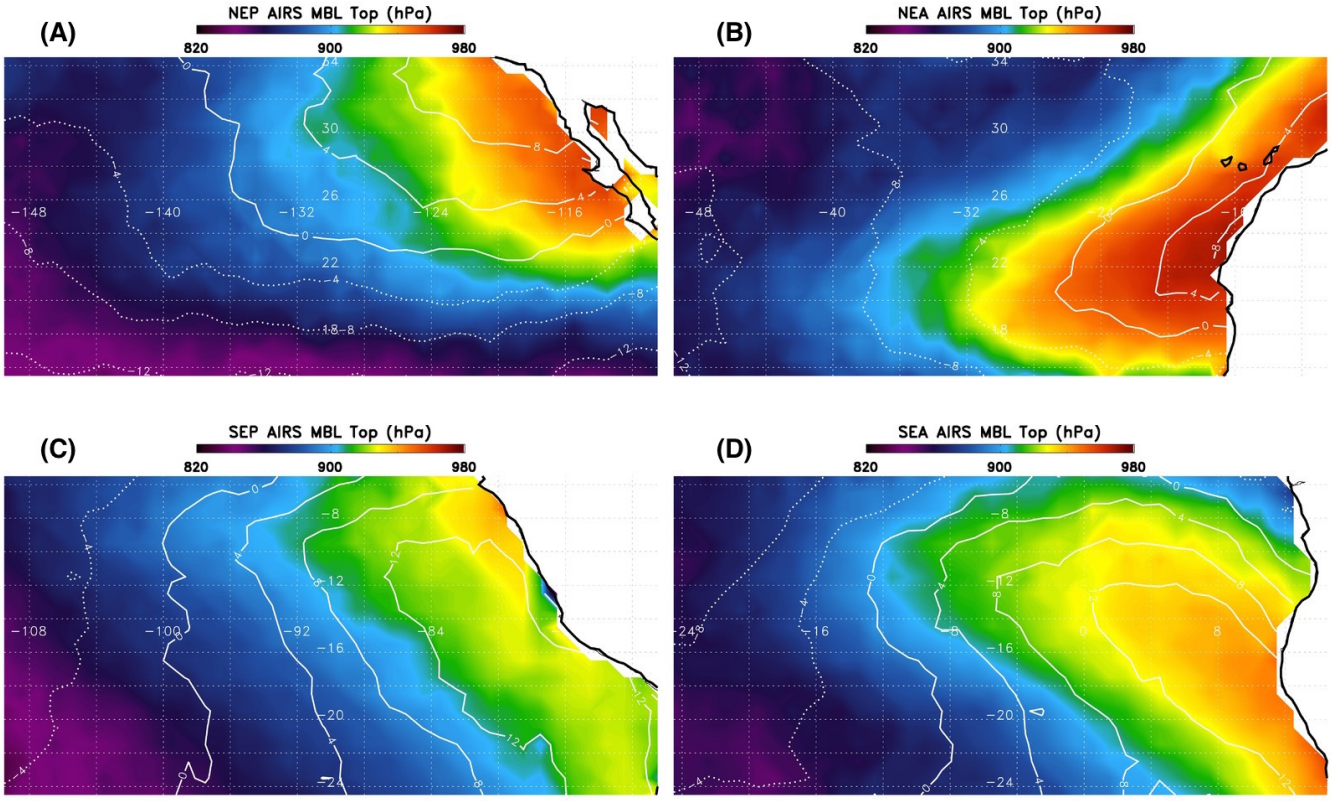

Figure 4. MBL depth (hPa) for regions listed in Table 1: (a) NEP, (b) NEA, (c), SEP, and (d) SEA. The AIRS 1000-700 hPa dMSE is overlaid in white contors (solid are for positive and dashed for negative).

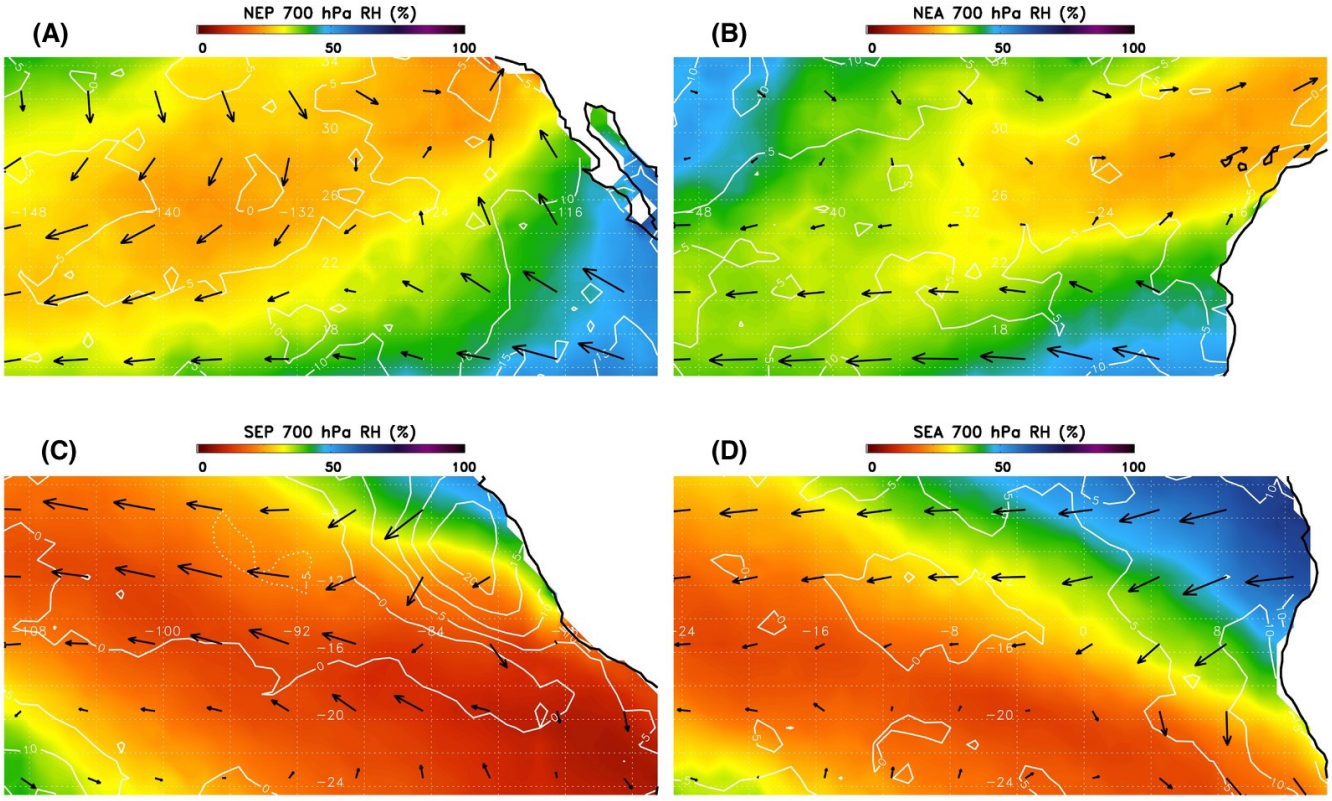

Figure 5. AIRS RH_{700} (%) for regions listed in Table 1: (a) NEP, (b) NEA, (c), SEP, and (d) SEA. The MERRA-AIRS RH_{700} difference is shown as white contours (solid implies MERRA is moister, and dashed implies AIRS is moister). The length and direction of the arrows depict the 700 hPa wind vectors from MERRA.

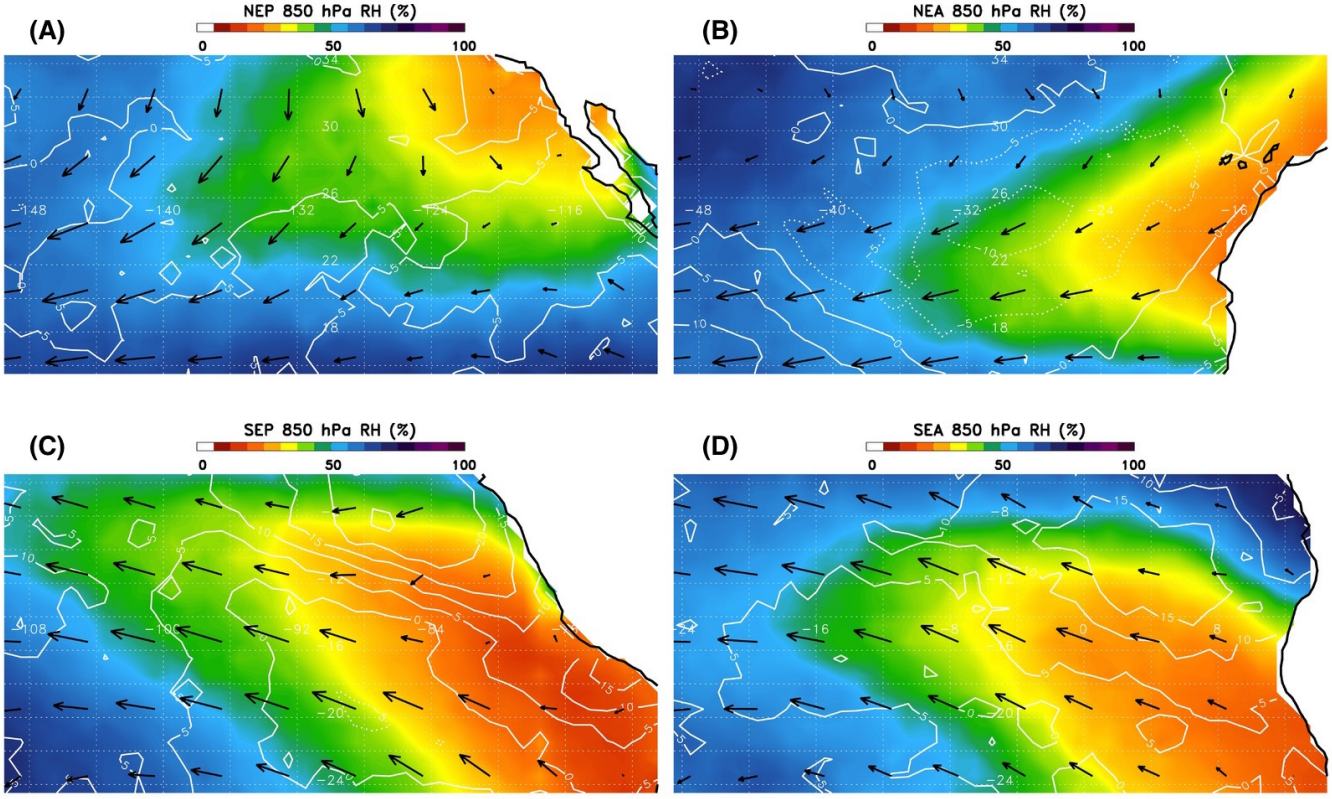

Figure 6. AIRS RH_{850} (%) for regions listed in Table 1: (a) NEP, (b) NEA, (c), SEP, and (d) SEA. The MERRA-AIRS RH_{850} difference is shown as white contours (solid implies MERRA is moister, and dashed implies AIRS is moister). The length and direction of the arrows depict the 850 hPa wind vectors from MERRA.

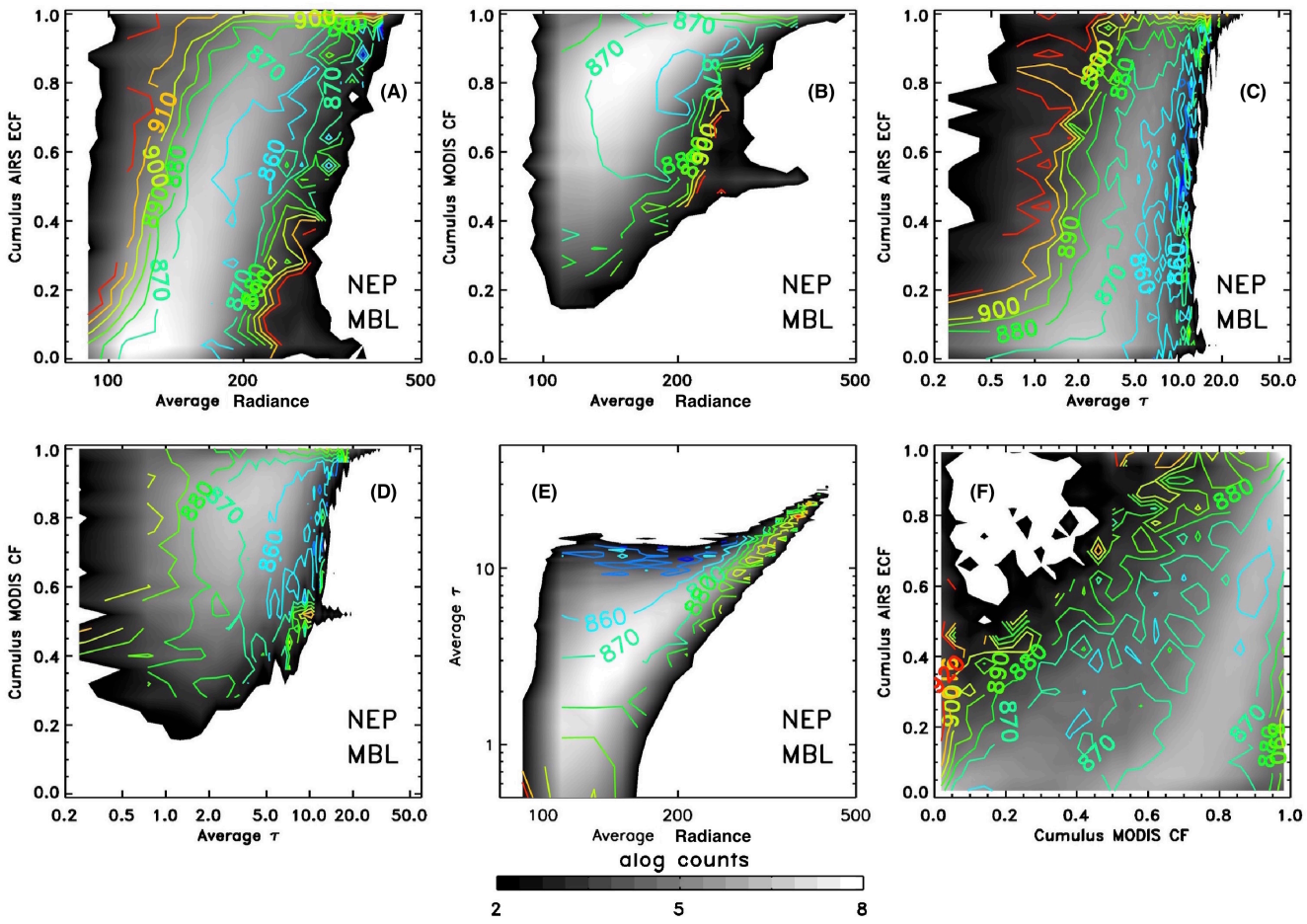

Figure 7. Shown are joint pdfs for six ~~four~~ different combinations of variables that are described in Section 4.2: (a) radiance ~~reflectance~~ versus AIRS ECF, (b) radiance ~~MODIS τ~~ versus MODIS CF ~~AIRS ECF~~, (c) MODIS τ ~~reflectance~~ versus AIRS ECF ~~MODIS cloud fraction~~, ~~and~~ (d) MODIS τ versus MODIS ~~CF cloud fraction~~, (e) radiance versus MODIS τ, and (f) MODIS CF versus AIRS ECF. The ~~black to~~ grey ~~to white~~ scale is the natural log of total counts per bin~~, where black is alog(counts)=2.0 and white is alog(counts)=8.0~~. All values in the pdfs shown are for the cumulus regime. The color contours depict the MBL depth (hPa).

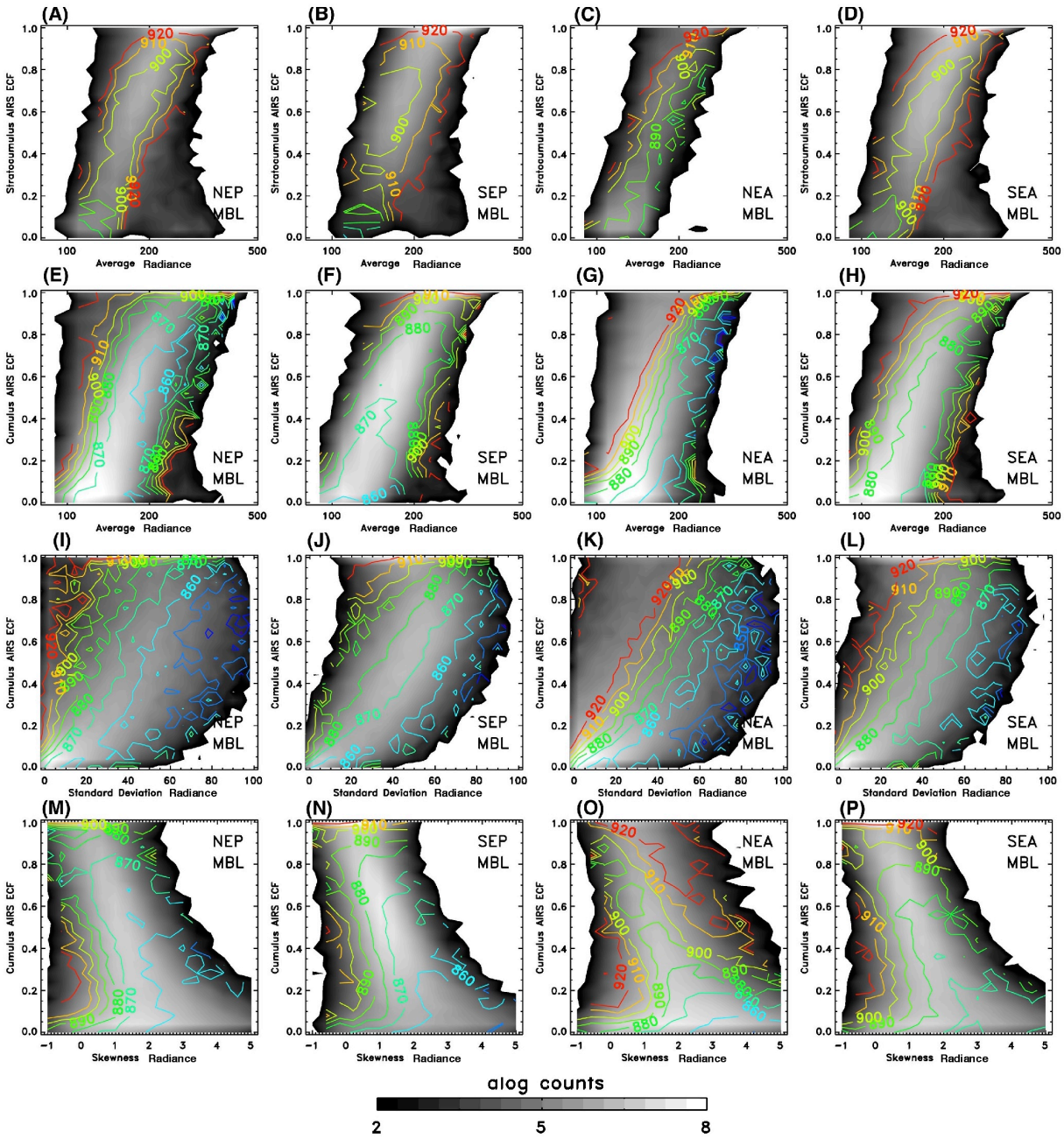

Figure 8. Joint pdfs of visible radiance ~~reflectance~~ versus ECF for the four spatial regions listed in Table 1. The SEP in Fig.7 is repeated here for clarity.

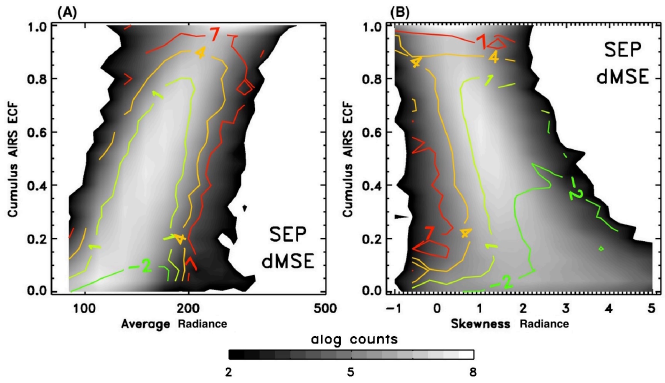

Figure 9. Joint pdfs of visible radiance ~~reflectance~~ average (left) and skewness (right) versus ECF for the SEP with dMSE depth as the overlay field. Other regions are very similar and are not shown for reasons of brevity.

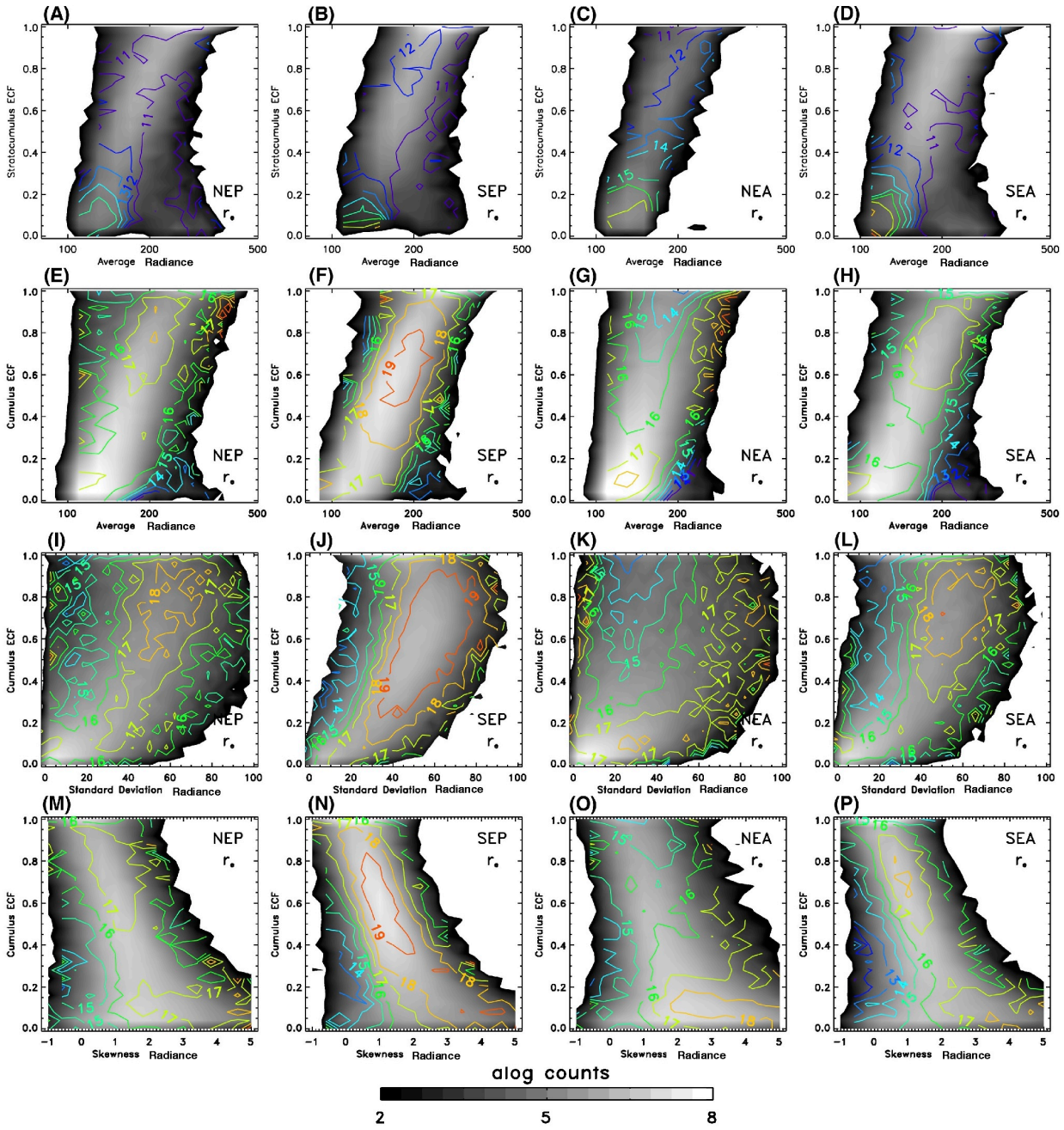

Figure 10 ~~11~~. Joint pdfs of visible radiance ~~reflectance~~ skewness versus ECF for the four regions listed in Table 1, and the overlay field is r_e.

5

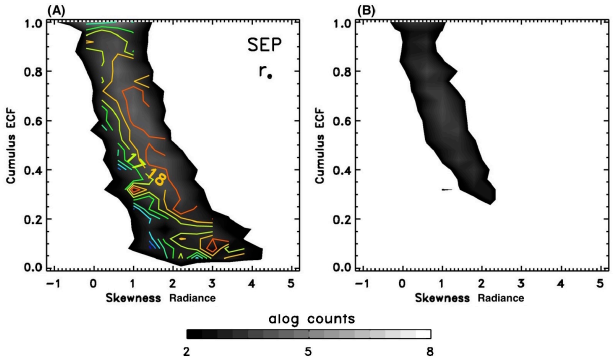

Figure 11 ~~12~~. (a) Same as Fig. 10~~12~~n except sampling restricted to AMSU FORs that contain the CloudSat ground track. (b) Samples of the data in (a) that contain detected precipitation according to CloudSat.

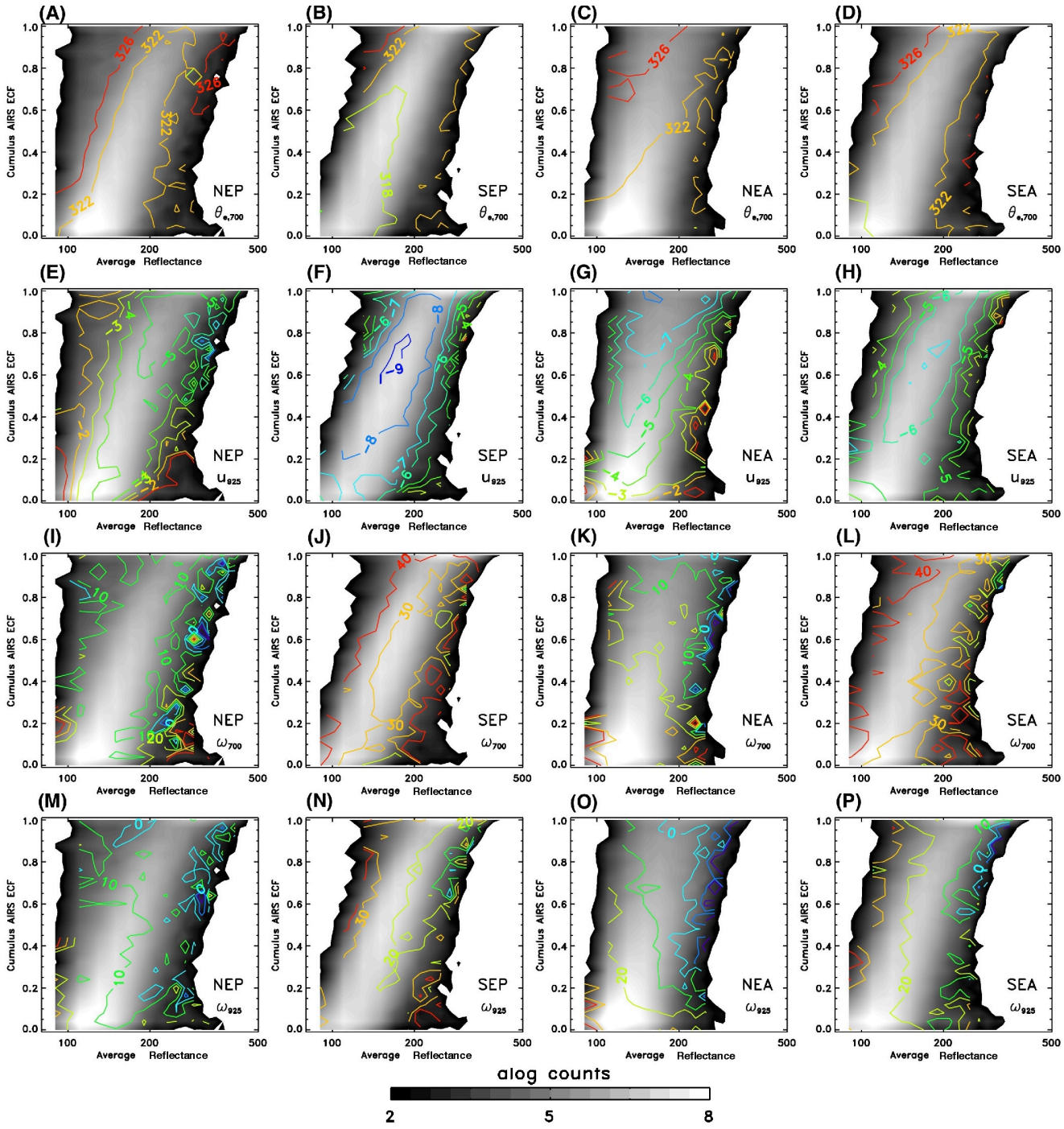

Figure 12 ~~13~~. Joint pdfs of 700 hPa θ_e, u_{925}, ω_{700}, and ω_{925}~~, theta, theta-e, u, and omega~~ for the four regions listed in Table 1.